

Orientation selectivity of affine Gaussian derivative based receptive fields

Tony Lindeberg

Abstract This paper presents a theoretical analysis of the orientation selectivity of simple and complex cells that can be well modelled by the generalized Gaussian derivative model for visual receptive fields, with the purely spatial component of the receptive fields determined by oriented affine Gaussian derivatives for different orders of spatial differentiation.

A detailed mathematical analysis is presented for the three different cases of either: (i) purely spatial receptive fields, (ii) space-time separable spatio-temporal receptive fields and (iii) velocity-adapted spatio-temporal receptive fields. Closed-form theoretical expressions for the orientation selectivity curves for idealized models of simple and complex cells are derived for all these main cases, and it is shown that the degree of orientation selectivity of the receptive fields increases with a scale parameter ratio κ , defined as the ratio between the scale parameters in the directions perpendicular to vs. parallel with the preferred orientation of the receptive field. It is also shown that the degree of orientation selectivity increases with the order of spatial differentiation in the underlying affine Gaussian derivative operators over the spatial domain.

We conclude by describing biological implications of the derived theoretical results, demonstrating that the predictions from the presented theory are consistent with previously established biological results concerning broad vs. sharp orientation tuning of visual neurons in the primary visual cortex. We also demonstrate that the above theoretical predictions, in combination with these biological results, are consistent with a previously formulated biological hypothesis, stating that the biological receptive field shapes should span the degrees of freedom in affine image transformations,

The support from the Swedish Research Council (contract 2022-02969) is gratefully acknowledged.

Computational Brain Science Lab, Division of Computational Science and Technology, KTH Royal Institute of Technology, SE-100 44 Stockholm, Sweden. E-mail: tony@kth.se

to support affine covariance over the population of receptive fields in the primary visual cortex.

Keywords Receptive field · Orientation selectivity · Affine covariance · Gaussian derivative · Quasi quadrature · Simple cell · Complex cell · Vision · Theoretical neuroscience

1 Introduction

The receptive fields in the primary visual cortex (V1) capture properties of the visual patterns, which are then passed on to higher layers in the visual hierarchy. Being able to understand the computational function of these receptive fields is hence essential for understanding the computational function of the visual system.

The task of understanding the visual system has been addressed both neurophysiologically, by measuring the response properties of neurons to visual stimuli, and by formulating mathematical models, that aim at both explaining the computational function of visual neurons, as well as enabling computational simulation of neural functions in terms of biologically plausible computer vision algorithms, or aiming at making theoretical predictions, which can then be investigated experimentally.

Hubel and Wiesel (1959, 1962, 2005) pioneered the study of visual neurons in the primary visual cortex, and introduced the taxonomy of simple and complex cells. Simple cells were simple characterized by their properties of (i) having distinct excitatory and inhibitory regions, (ii) obeying roughly linear summation properties, (iii) the excitatory and inhibitory regions balance each other in diffuse lighting. Visual neurons that did not obey these properties were referred to as complex cells. The response of a complex cell to a visual stimulus was also reported to be much less sensitive to the position of the stimulus in the visual field than for a simple cell.

More detailed characterizations of the receptive fields of simple cells have then been performed by DeAngelis *et al.* (1995, 2004), Ringach (2002, 2004), Conway and Livingstone (2006), Johnson *et al.* (2008) and De and Horwitz (2021), where specifically the use of multiple white noise stimuli permit a reconstruction of the full receptive field of a visual neuron, based on theoretical results in system identification theory, assuming linearity of the neuron. Furthermore, more detailed characterizations of the orientation selectivity of visual neurons have been performed by Rose and Blakemore (1974), Schiller *et al.* (1976), Ringach *et al.* (2002), Nauhaus *et al.* (2008), Scholl *et al.* (2013) and Goris *et al.* (2015).

Mathematical models of simple cells have been formulated, in terms of Gabor filters (Marcelja 1980; Jones and Palmer 1987a, 1987b; Porat and Zeevi 1988) or Gaussian derivatives (Koenderink and van Doorn 1984, 1987, 1992; Young and his co-workers 1987, 2001, 2001, Lindeberg 2013, 2021). Specifically, theoretical models of early visual processes in terms of Gaussian derivatives have been formulated by Lowe (2000), May and Georgeson (2007), Hesse and Georgeson (2005), Georgeson *et al.* (2007), Wallis and Georgeson (2009), Hansen and Neumann (2008), Wang and Spratling (2016) and Pei *et al.* (2016).

Beyond the work by Hubel and Wiesel, the properties of complex cells have been further characterized by Movshon *et al.* (1978), Emerson *et al.* (1987), Touyan *et al.* (2002, 2005), Rust *et al.* (2005) and Goris *et al.* (2015), as well as modelled computationally by Adelson and Bergen (1985), Heeger (1992), Serre and Riesenhuber (2004), Einhäuser *et al.* (2002), Kording *et al.* (2004), Merolla and Boahen (2004), Berkes and Wiskott (2005), Carandini (2006) and Hansard and Horoud (2011).

The subject of this paper is to perform a detailed analysis of the orientation selectivity properties of models of simple and complex cells based on image measurements in terms of affine Gaussian derivatives. The notion of affine Gaussian smoothing, with its associated notion of affine Gaussian derivatives, was derived axiomatically in (Lindeberg 2011) and was proposed as a spatial model of simple cells in (Lindeberg 2013, 2021). This model has also been extended to complex cells in (Lindeberg 2020 Section 5). Parallel extensions of the affine Gaussian derivative model for simple cells to spatio-temporal receptive fields have been performed in (Lindeberg 2016, 2021).

In this paper, we will build upon these latter works and perform an in-depth analysis of the orientation selectivity curves that result from the associated models of receptive fields for simple and complex cells. Specifically, we will focus on quantifying how the degree of orientation selectivity of a receptive field depends on how anisotropic the underlying affine Gaussian derivatives are. We will derive explicit expressions for how the degree of orientation selec-

tivity increases with the ratio between the scale parameters in the orientations perpendicular to *vs.* parallel with the preferred orientation of the receptive fields. In this way, we also demonstrate how closed form theoretical analysis is possible for generalized Gaussian derivative model for visual receptive fields, which arises from the normative theory of visual receptive fields in (Lindeberg 2021).

We will then use these theoretical results to provide indirect support for a biological hypothesis raised in (Lindeberg 2023), concerning how the variability of the shapes of receptive fields may be related to the variability of image structures under natural image transformations. If we assume that the visual system should implement affine covariant receptive fields, to make it possible for the visual system to better estimate shape properties of surfaces in the world, such as local surface orientation, then the property of affine covariance would make it possible to compute better estimates of local surface orientation, compared to a visual system that does not implement affine covariance, or a sufficiently good approximation thereof.

If we further assume that the spatial components of the receptive fields can be well modelled by affine Gaussian derivatives, then the property of affine covariance implies that there should be visual receptive fields for different degrees of anisotropy present in the visual system. If we further combine the theoretical results derived in this paper, which will state that the degree of orientation selectivity is strongly dependent on the anisotropy of the receptive fields, with the biological results established by Nauhaus *et al.* (2008), which show that the degree of orientation selectivity for neurons in the primary visual cortex depends strongly with the position on the cortical surface in relation to the pinwheels, then these results together are fully consistent with the hypothesis that the visual receptive fields in the primary visual cortex should have a variability in their anisotropy, thus consistent with the hypothesis that the receptive fields in the pinwheel structure should span at least one more degree of freedom in the affine group, beyond mere rotations, as already established in the pinwheel structure of the oriented receptive fields in the primary visual cortex.

1.1 Structure of this article

This paper is organized as follows: Section 2 gives a theoretical background to this work, by describing the generalized Gaussian derivative model for visual receptive fields, both in the cases of a purely spatial domain, where the receptive fields are pure affine Gaussian derivatives, and for a joint spatio-temporal domain, where the affine Gaussian derivatives are complemented by temporal derivatives of either a non-causal Gaussian kernel over the temporal domain, or a genuine time-causal kernel, referred to as the time-causal

limit kernel, as well as complemented with possible velocity adaptation, to enable Galilean covariance.

Beyond these models of simple cells, we do both review a previously formulated purely spatial model for complex cells, based on a Euclidean combination of scale-normalized affine Gaussian derivatives of orders 1 and 2, as well as propose two new spatio-temporal models for complex cells, based on image measurements in terms of affine Gaussian derivatives over the spatial domain, complemented by explicit temporal processing operations. Two special cases are treated in terms of either space-time separable spatio-temporal receptive fields, or velocity-adapted spatio-temporal receptive fields, with the latter tuned to particular motion directions and motion velocities in joint space-time.

Section 3 then performs a detailed mathematical analysis of the orientation selectivity of these models, over three main cases of either (i) a purely spatial domain, (ii) a space-time separable spatio-temporal domain, or (iii) a velocity-adapted spatio-temporal domain. In each of these main cases, we analyze the properties of simple cells of orders 1 and 2, corresponding to first- or second-order Gaussian derivatives, as well as the orientation selectivity properties for our models of complex cells.

Concerning simple cells, it is shown that both the pure spatial receptive fields and the joint spatio-temporal receptive fields have similar orientation selectivity properties, which only depend on the order of spatial differentiation and the degree of anisotropy of the receptive field. For complex cells, a different dependency is, however, derived for the model based on space-time separable receptive fields, as opposed to the models for either a purely spatial domain or a joint spatio-temporal domain, based on velocity-adapted spatio-temporal receptive fields.

Section 4 then develops implications of the presented theoretical results for biological vision. Comparisons are made to previous work by Nauhaus *et al.* (2008), concerning relations between the degree of orientation selectivity of biological receptive fields and the positions of the corresponding neurons on the cortical surface in the primary visual cortex, in relation to the pinwheel structure.

Specifically, it is demonstrated that the predictions generated from the presented theory are consistent with the experimentally observed biological facts concerning broad orientation tuning of the receptive fields near the pinwheels and sharper orientation tuning further away. These variations in the degree of orientation selectivity are, in turn, consistent with the variations in the degree of orientation selectivity in our idealized models of receptive fields, under variations in the parameter κ , or its inverse entity, the eccentricity $\epsilon = 1/\kappa$.

By combining our theoretical predictions with the experimental measurements of biological orientation selectivity, we argue that these similarities can serve as indirect support

for the hypothesis that the shapes of visual receptive fields in the primary visual cortex should comprise a variability over the parameter κ (or ϵ) in the to support affine covariance of the family of receptive fields, to, in turn, enable more accurate determinations of cues to the 3-D structure of the world, such as estimates of local surface orientation.

Finally, Section 5 gives a summary and discussion about some of the main results, including suggestions concerning possible extensions of the presented work.

2 Receptive field models based on affine Gaussian derivatives

For modelling the response properties of simple cells, we will in this paper make use of the affine Gaussian derivative model for linear receptive fields, which has been theoretically derived in a principled axiomatic manner in (Lindeberg 2011), and then been demonstrated in (Lindeberg 2013, 2021) to well model the spatial properties of simple cells in the primary cortex, as established by neurophysiological measurements by DeAngelis *et al.* (1995, 2004) and Johnson *et al.* (2008); see Figures 16–17 in (Lindeberg 2021) for comparisons between biological receptive fields and computational models in terms of affine Gaussian derivatives, as will be used as a basis for the analysis in this paper.

In this section, we shall define the affine Gaussian derivative model for simple cells over a purely spatial domain, as well as a corresponding generalized affine Gaussian derivative model for simple cells over a joint spatio-temporal domain. Based on these models of simple cells, we shall then also define models for complex cells, both over a purely spatial image domain and over a joint spatio-temporal domain.

2.1 Purely spatial model of simple cells

If we initially disregard the temporal dependencies of the simple cells, we can formulate a purely spatial model of linear receptive fields with orientation preference according to (Lindeberg 2021 Equation (23)), see (Lindeberg 2021 Figure 7) for illustrations of such receptive fields;

$$\begin{aligned} T_{\text{simple}}(x_1, x_2; \sigma_\varphi, \varphi, \Sigma_\varphi, m) \\ = T_{\varphi^m, \text{norm}}(x_1, x_2; \sigma_\varphi, \Sigma_\varphi) = \sigma_\varphi^m \partial_\varphi^m (g(x_1, x_2; \Sigma_\varphi)), \end{aligned} \quad (1)$$

where

- φ represents the preferred orientation of the receptive field,

- σ_φ represents the amount of spatial smoothing¹ in the direction φ (in units of the spatial standard deviation²),
- $\partial_\varphi^m = (\cos \varphi \partial_{x_1} + \sin \varphi \partial_{x_2})^m$ is an m :th-order directional derivative operator³ in the direction φ ,
- Σ_φ is a symmetric positive definite covariance matrix, with one of its eigenvectors aligned with the direction of φ , and
- $g(x; \Sigma_\varphi)$ is a 2-D affine Gaussian kernel with its shape determined by the covariance matrix Σ_φ

$$g(x; \Sigma_\varphi) = \frac{1}{2\pi\sqrt{\det \Sigma_\varphi}} e^{-x^2 \Sigma_\varphi^{-1} x/2} \quad (2)$$

for $x = (x_1, x_2)^T$, and with one of the eigenvectors of Σ_φ parallel to the orientation φ .

In the above expression for the spatial receptive field model T_{simple} , the multiplication of the m :th-order directional derivative operator in the direction φ by the spatial scale parameter σ_φ in the same direction, implements scale-normalized derivatives (Lindeberg 1998) according to

$$\partial_{x_1^{\alpha_1} x_2^{\alpha_2}, norm} = \sigma^{\gamma(\alpha_1 + \alpha_2)} \partial_{x_1^{\alpha_1} x_2^{\alpha_2}}, \quad (3)$$

where we here, for simplicity, choose the scale normalization power $\gamma = 1$ to simplify the following calculations.

This notion of spatial scale-normalized derivatives implies that we measure the amplitude of local spatial variations with respect to a given scale level, and makes it possible to define scale-invariant feature responses, that assume the same magnitude for input image structures of different spatial extent, provided that the spatial scale levels are adapted to the characteristic length of spatial variations in the image data. Specifically, this spatial scale normalization of the spatial receptive field response implies scale selective properties in the sense that the receptive field will produce

¹ If we let e_φ denote the unit vector in the direction of φ , according to $e_\varphi = (\cos \varphi, \sin \varphi)^T$, then we can determine σ_φ from the spatial covariance matrix Σ_φ according to $\sigma_\varphi = \sqrt{e_\varphi^T \Sigma_\varphi e_\varphi}$.

² In this paper, we parameterize both the spatial and the temporal scale parameters in units of the standard deviations of the corresponding spatial or temporal smoothing kernels. These parameters are related to the corresponding variance-based parameterizations in the earlier work, that we build upon, according to $\sigma_{space} = \sqrt{s}$ and $\sigma_{time} = \sqrt{\tau}$. By this change of notation, some equations in this paper will have somewhat different appearance, compared to the previous work that we cite. This change of notation will, however, lead to easier notation in the mathematical analysis that will follow in Section 3

³ Concerning the notation, we write derivatives either in operator form ∂_{x_1} , which constitutes short notation for $\frac{\partial}{\partial x_1}$, or as subscripts, $L_{x_1} = \partial_{x_1} L$, which is also short notation for $\frac{\partial L}{\partial x_1}$. Directional derivatives of functions are also written as subscripts $L_\varphi = \partial_\varphi L$ and can, of course, also be applied repeatedly $L_{\varphi\varphi} = \partial_\varphi^2 L$. Observe, however, that subscripts are also used with a different meaning in connections constants. The notation σ_φ means the σ -value used when computing directional derivatives, as opposed to σ_t , to be introduced later, which means the σ -value that is used when computing temporal derivatives.

its maximum response over spatial scales at a spatial scale proportional to a characteristic length in the image data.

Note that this model for the spatial dependency of simple cells, in terms of affine Gaussian derivatives, goes beyond the previous biological modelling results by Young (1987), in turn with very close relations to theoretical modelling results by Koenderink and van Doorn (1987, 1992), in that the spatial smoothing part of the receptive field is here spatially anisotropic, and thereby allows for higher orientation selectivity compared to defining (regular) Gaussian derivatives from partial derivatives or directional derivatives of rotationally symmetric Gaussian kernels, as used by Young and Koenderink and van Doorn. Direct comparisons with biological receptive fields, see Figures 16–17 in (Lindeberg 2021), also show that biological simple cells are more anisotropic than can be well modelled by directional derivatives of rotationally symmetric Gaussian kernels.

2.2 Purely spatial model of complex cells

In (Lindeberg 2020 Section 5) it was proposed that some of the qualitative properties of complex cells, of being both (i) polarity-independent, (ii) approximately phase-independent and (ii) not obeying a superposition principle, as opposed to polarity-dependent as well as strongly phase-dependent, as simple cells are, can be modelled by combining first- and second-order directional affine Gaussian derivative responses of the form⁴

$$Q_{\varphi, spat, norm} L = \sqrt{\frac{L_{\varphi, norm}^2 + C_\varphi L_{\varphi\varphi, norm}^2}{\sigma_\varphi^{2\Gamma}}}, \quad (4)$$

where

- $L_{\varphi, norm}$ and $L_{\varphi\varphi, norm}$ represent the results of applying scale-normalized directional affine Gaussian derivative operators of orders 1 and 2, respectively, according to (1), to the input image f :

$$L_{\varphi, norm}(x_1, x_2; \sigma_\varphi, \Sigma_\varphi) = \\ = T_{\varphi, norm}(x_1, x_2; \sigma_\varphi, \Sigma_\varphi) * f(x_1, x_2), \quad (5)$$

$$L_{\varphi\varphi, norm}(x_1, x_2; \sigma_\varphi, \Sigma_\varphi) = \\ = T_{\varphi\varphi, norm}(x_1, x_2; \sigma_\varphi, \Sigma_\varphi) * f(x_1, x_2), \quad (6)$$

- $C_\varphi > 0$ is a weighting factor between first and second-order information, and

⁴ In the expressions below, the symbol L denotes the result of pure spatial smoothing of the input image $f(x_1, x_2)$ with an affine Gaussian kernel $g(x_1, x_2; \Sigma)$, i.e., $L(x_1, x_2; \Sigma) = g(x_1, x_2; \Sigma) * f(x_1, x_2)$. In the area of scale-space theory, this representation is referred to as the (affine) spatial scale-space representation of f .

- $\Gamma \geq 0$ is a complementary scale normalization parameter, that we, however, henceforth will set to zero, to simplify the following treatment.

This model is can be seen as an affine Gaussian derivative analogue of the energy model of complex cells proposed by Adelson and Bergen (1985) and Heeger (1992), specifically the fact that receptive fields similar to first- vs. second-order derivatives are reported to occur in pairs (De Valois *et al.* 2000), resembling properties of approximate quadrature pairs, as related by a Hilbert transform (Bracewell 1999, pp. 267–272). The model is also closely related to the proposal by Koenderink and van Doorn (1990) to sum up the squares of first- and second-order derivative response, in a corresponding way as cosine wave and sine wave responses are combined in a Euclidean manner, to get a more phase-independent response.

For a perfect quadrature pair of filters, the sum of the squares of the filter responses will be spatially constant for any sine wave of any frequency and phase. The quasi quadrature entity will instead have the property that the response will be spatially constant, or alternatively have only relatively moderate ripples, at or near the spatial scale level at which the quasi quadrature measure assumes its maximum value over spatial scales, provided that the value of the weighting parameter C_φ is properly chosen. In this way, the quasi quadrature measure combines the responses of the first- and second-order affine Gaussian derivative operators in a complementary manner, where the first-order derivatives correspond to odd filters (antisymmetric under reflection) and the second-order derivatives to even filters (symmetric under reflection).

2.3 Joint spatio-temporal models of simple cells

For modelling the joint spatio-temporal behaviour of linear receptive fields with orientation preference, in (Lindeberg 2021 Section 3.2) the following model is derived from theoretical arguments, see (Lindeberg 2021 Figures 10-11 for illustrations)

$$\begin{aligned} T_{\text{simple}}(x_1, x_2, t; \sigma_\varphi, \sigma_t, \varphi, v, \Sigma_\varphi, m, n) \\ = T_{\varphi^m, \bar{t}^n, \text{norm}}(x_1, x_2, t; \sigma_\varphi, \sigma_t, v, \Sigma_\varphi) \\ = \sigma_\varphi^m \sigma_t^n \partial_\varphi^m \partial_t^n (g(x_1 - v_1 t, x_2 - v_2 t; \Sigma_\varphi) h(t; \tau)), \end{aligned} \quad (7)$$

where (for symbols not previously defined in connection with Equation (1))

- σ_t represents the amount of temporal smoothing (in units of the temporal standard deviation),
- $v = (v_1, v_2)^T$ represents a local motion vector, in the direction φ of the spatial orientation of the receptive field,

- $\partial_t^n = (\partial_t + v_1 \partial_{x_1} + v_2 \partial_{x_2})^n$ represents an n :th-order velocity-adapted temporal derivative operator,
- $h(t; \sigma_t)$ represents a temporal smoothing kernel with temporal standard deviation σ_t .

In the case of non-causal time (where the future can be accessed), the temporal kernel can be determined to be a 1-D Gaussian kernel

$$h(t; \sigma_t) = \frac{1}{\sqrt{2\pi}\sigma_t} e^{-t^2/2\sigma_t^2}, \quad (8)$$

whereas in the case of time-causal time (where the future cannot be accessed), the temporal kernel can instead be chosen as the time-causal limit kernel (Lindeberg 2016 Section 5)

$$h(t; \sigma_t) = \psi(t; \sigma_t, c), \quad (9)$$

defined by having a Fourier transform of the form

$$\hat{\Psi}(\omega; \sigma_t, c) = \prod_{k=1}^{\infty} \frac{1}{1 + i c^{-k} \sqrt{c^2 - 1} \sigma_t \omega}, \quad (10)$$

and corresponding to an infinite set of first-order integrators coupled in cascade with specifically chosen time constants to enable temporal scale covariance, where the distribution parameter c describes the ratio between adjacent discrete temporal scale levels in this temporal scale-space model.

In analogy with the spatial scale normalization in the previous purely spatial model, multiplication of the n :th-order velocity-adapted temporal derivative operator ∂_t^n by the temporal standard deviation σ_t raised to the power of n implements scale-normalized velocity-adapted temporal derivatives according to

$$\partial_{t, \text{norm}}^n = \sigma_t^{\gamma n} \partial_t^n, \quad (11)$$

as an extension of Equation (3) from the spatial to the temporal domain, see (Lindeberg 2017). Also here, for simplicity, we restrict ourselves to the specific choice of the scale normalization parameter $\gamma = 1$. By this temporal scale normalization, the temporal component of the spatio-temporal receptive field will have scale selective properties, implying that it will produce its maximum response over temporal scales at a temporal scale proportional to a characteristic temporal duration of the temporal structures in the video data.

In Figure 18 in (Lindeberg 2021) it is demonstrated that this model well captures the qualitative properties of simple cells in the primary visual cortex, as established by neurophysiological cell recordings by DeAngelis *et al.* (1995, 2004), regarding both space-time separable receptive fields and velocity-adapted receptive fields, tuned to particular motion directions in joint space-time.

Note that these spatio-temporal models of simple cells go beyond the previous biological modelling results by Young

and his co-workers (2001, 2001) in that: (i) the purely spatial smoothing component of the receptive field model is based on anisotropic Gaussian kernels as opposed to rotationally symmetric Gaussian kernels, (ii) this model also incorporates a truly time-causal model, that takes into explicit account that the future cannot be accessed in a real-world situation, and (iii) the parameterization of the spatio-temporal filter shapes is different, and more closely aligned to the inherent geometry of the imaging situation.

2.4 Joint spatio-temporal models of complex cells

2.4.1 Model based on space-time separable receptive fields

For modelling qualitative properties of complex cells over the joint spatio-temporal domain, we can extend the quasi quadrature measure in (4) to also operate on a combination of spatial directional derivatives and temporal derivatives according to

$$\begin{aligned} (\mathcal{Q}_{\varphi,sep,norm} L)^2 = & ((L_{\varphi,t,norm}^2 + C_t L_{\varphi,tt,norm}^2) \\ & + C_\varphi (L_{\varphi\varphi,t,norm}^2 + C_t L_{\varphi\varphi,tt,norm}^2)) / (\sigma_\varphi^{2\Gamma_\varphi} \sigma_t^{2\Gamma_t}), \end{aligned} \quad (12)$$

where the individual components in this expression are defined from space-time separable receptive fields according to

$$\begin{aligned} L_{\varphi,t,norm}(x_1, x_2, t; \sigma_\varphi, \sigma_t, 0, \Sigma_\varphi) = \\ = T_{\varphi,t,norm}(x_1, x_2, t; \sigma_\varphi, \sigma_t, 0, \Sigma_\varphi) * f(x_1, x_2, t), \end{aligned} \quad (13)$$

$$\begin{aligned} L_{\varphi,tt,norm}(x_1, x_2, t; \sigma_\varphi, \sigma_t, 0, \Sigma_\varphi) = \\ = T_{\varphi,tt,norm}(x_1, x_2, t; \sigma_\varphi, \sigma_t, 0, \Sigma_\varphi) * f(x_1, x_2, t), \end{aligned} \quad (14)$$

$$\begin{aligned} L_{\varphi\varphi,t,norm}(x_1, x_2, t; \sigma_\varphi, \sigma_t, 0, \Sigma_\varphi) = \\ = T_{\varphi\varphi,t,norm}(x_1, x_2, t; \sigma_\varphi, \sigma_t, 0, \Sigma_\varphi) * f(x_1, x_2, t), \end{aligned} \quad (15)$$

$$\begin{aligned} L_{\varphi\varphi,tt,norm}(x_1, x_2, t; \sigma_\varphi, \sigma_t, 0, \Sigma_\varphi) = \\ = T_{\varphi\varphi,tt,norm}(x_1, x_2, t; \sigma_\varphi, \sigma_t, 0, \Sigma_\varphi) * f(x_1, x_2, t), \end{aligned} \quad (16)$$

with the underlying space-time separable spatio-temporal receptive fields $T_{\varphi^m, t^n, norm}(x_1, x_2, t; \sigma_\varphi, \sigma_t, 0, \Sigma_\varphi)$ according to (7) for $v = 0$.

In the expression (12), the quasi quadrature measure operates on both pairs of first- and second-order directional derivatives as well as pairs of first- and second-order velocity-adapted derivatives simultaneously, aimed at balancing the

responses of odd *vs.* even filter responses over both space or time in parallel.

This spatio-temporal quasi quadrature measure constitutes an extension of the spatio-temporal quasi quadrature measure in (Lindeberg 2018 Section 4.2), by being additionally adapted to be selective to particular image orientations over the spatial domain, as opposed to being rotationally isotropic, as well as being based on affine Gaussian derivative operators, as opposed to partial derivatives of rotationally symmetric Gaussian kernels over the spatial domain.

This oriented spatio-temporal quasi quadrature measure will specifically inherit the qualitative properties of the previously presented purely spatial oriented quasi quadrature measure (33) in that it will be polarity-independent as well as much less sensitive to the phase in the input video data compared to the above models of simple cells.

2.4.2 Model based on velocity-adapted receptive fields

If we would compute the above spatio-temporal quasi quadrature measure based on velocity-adapted spatio-temporal receptive fields, then the quasi quadrature measure would be zero if the velocity vector of the velocity-adapted receptive fields is equal to the velocity-value of the moving sine wave pattern. To define a quasi quadrature measure that instead will give a maximally strong response if the velocity vector is adapted to the velocity vector of a moving pattern, we do therefore instead define a quasi quadrature measure for velocity-adapted receptive fields by extending the purely spatial quasi quadrature measure (4) to operate on spatial receptive fields complemented by a temporal smoothing stage, *i.e.*, velocity-adapted receptive fields for zero order of temporal differentiation ($n = 0$ in (7)):

$$(\mathcal{Q}_{\varphi,vel,norm} L) = \sqrt{\frac{L_{\varphi,norm}^2 + C_\varphi L_{\varphi\varphi,norm}^2}{\sigma_\varphi^{2\Gamma}}}, \quad (17)$$

where the individual components in this expression are defined from space-time separable receptive fields according to

$$\begin{aligned} L_{\varphi,norm}(x_1, x_2, t; \sigma_\varphi, \sigma_t, v, \Sigma_\varphi) = \\ = T_{\varphi,norm}(x_1, x_2, t; \sigma_\varphi, \sigma_t, v, \Sigma_\varphi) * f(x_1, x_2, t), \end{aligned} \quad (18)$$

$$\begin{aligned} L_{\varphi\varphi,norm}(x_1, x_2, t; \sigma_\varphi, \sigma_t, v, \Sigma_\varphi) = \\ = T_{\varphi\varphi,norm}(x_1, x_2, t; \sigma_\varphi, \sigma_t, v, \Sigma_\varphi) * f(x_1, x_2, t), \end{aligned} \quad (19)$$

with the underlying space-time separable spatio-temporal receptive fields $T_{\varphi^m, t^n, norm}(x_1, x_2, t; \sigma_\varphi, \sigma_t, v, \Sigma_\varphi)$ according to (7) for $n = 0$.

Again, the intention behind this definition is that also this spatio-temporal quasi quadrature measure should be both polarity-independent with respect to the input and much less

sensitive to the phase in the input compared to the velocity-adapted spatio-temporal models of simple cells, while also in conceptual agreement with the energy models of complex cells.

3 Orientation selectivity for models of simple cells and complex cells

In this section, we will theoretically analyze the orientation selectivity properties of the above purely spatial as well as joint spatio-temporal models for receptive fields, when exposed to sine wave patterns with different orientations in relation to the preferred orientation of the receptive field.

For simplicity of analysis, and without loss of generality, we will henceforth align the coordinate system with the preferred orientation of the receptive field, in other words choosing the coordinate system such that the orientation angle $\varphi = 0$. Then, we will expose this receptive field to static as well as moving sine wave patterns, that are oriented with respect to an angle θ relative to the resulting horizontal x_1 -direction, as shown in Figure 1.

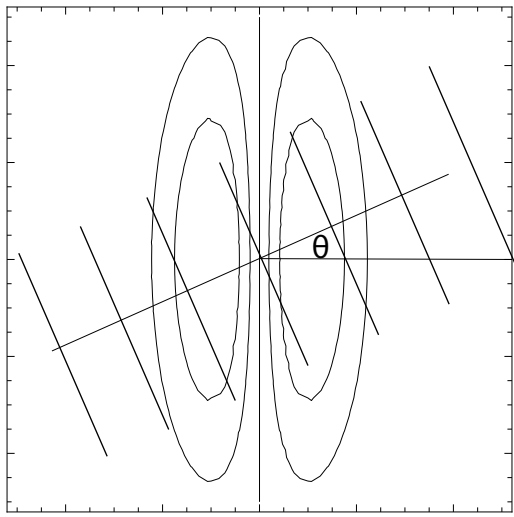


Fig. 1 Schematic illustration of the modelling situation studied in the theoretical analysis, where the coordinate system is aligned to the preferred orientation $\varphi = 0$ of the receptive field, and then exposed to a sine wave pattern with inclination angle θ . In this figure, the sine wave pattern is schematically illustrated by a set of level lines, overlayed onto a few level curves of a first-order affine Gaussian derivative.

By necessity, the presentation that will follow will be somewhat technical, since we will analyze the properties of our mathematical models for the receptive fields of simple and complex cells for three different main cases of either (i) purely spatial receptive fields, (ii) space-time separable spatio-temporal receptive fields and (iii) velocity-adapted spatio-temporal receptive fields.

The very hasty reader, who may be more interested in the final results only and their biological implications, while not in the details of the mathematical modelling with its associated theoretical analysis, can without major loss of continuity proceed directly to Section 3.4, where a condensed overview is given of the derived orientation selectivity results. The reader who additionally is interested in getting a brief overview of how the theoretical analysis is carried out, and the assumptions regarding the probing of the receptive fields that it rests upon, would be recommended to additionally read at least one of the theoretical modelling cases, where the purely spatial analysis in the following Section 3.1 then is the simplest one.

3.1 Analysis for purely spatial models of receptive fields

For the forthcoming purely spatial analysis, we will analyze the response properties of our spatial models of simple and complex cells to sine wave patterns with angular frequency ω and orientation θ of the form

$$f(x_1, x_2) = \sin(\omega \cos \theta x_1 + \omega \sin \theta x_2 + \beta). \quad (21)$$

3.1.1 First-order simple cell

Consider a simple cell that is modelled as a first-order scale-normalized derivative of an affine Gaussian kernel (according to (1) for $m = 1$), and oriented in the horizontal x_1 -direction (for $\varphi = 0$) with spatial scale parameter σ_1 in the horizontal x_1 -direction and spatial scale parameter σ_2 in the vertical x_2 -direction, and thus a spatial covariance matrix of the form $\Sigma_0 = \text{diag}(\sigma_1^2, \sigma_2^2)$:

$$\begin{aligned} T_{0,norm}(x_1, x_2; \sigma_1, \sigma_2) &= \\ &= \frac{\sigma_1}{2\pi\sigma_1\sigma_2} \partial_{x_1} \left(e^{-x_1^2/2\sigma_1^2 - x_2^2/2\sigma_2^2} \right) \\ &= -\frac{x_1}{2\pi\sigma_1^2\sigma_2} e^{-x_1^2/2\sigma_1^2 - x_2^2/2\sigma_2^2}. \end{aligned} \quad (22)$$

The corresponding receptive field response is then, after solving the convolution integral in Mathematica,

$$\begin{aligned} L_{0,norm}(x_1, x_2; \sigma_1, \sigma_2) &= \\ &= \int_{\xi_1=-\infty}^{\infty} \int_{\xi_2=-\infty}^{\infty} T_{0,norm}(\xi_1, \xi_2; \sigma_1, \sigma_2) \\ &\quad \times f(x_1 - \xi_1, x_2 - \xi_2) d\xi_1 d\xi_2 \\ &= \omega \sigma_1 \cos \theta e^{-\frac{1}{2}\omega^2(\sigma_1^2 \cos^2 \theta + \sigma_2^2 \sin^2 \theta)} \\ &\quad \times \cos(\omega \cos \theta x_1 + \omega \sin \theta x_2 + \beta), \end{aligned} \quad (23)$$

i.e., a cosine wave with amplitude

$$A_{\varphi}(\theta, \omega; \sigma_1, \sigma_2) = \omega \sigma_1 |\cos \theta| e^{-\frac{1}{2}\omega^2(\sigma_1^2 \cos^2 \theta + \sigma_2^2 \sin^2 \theta)}.$$

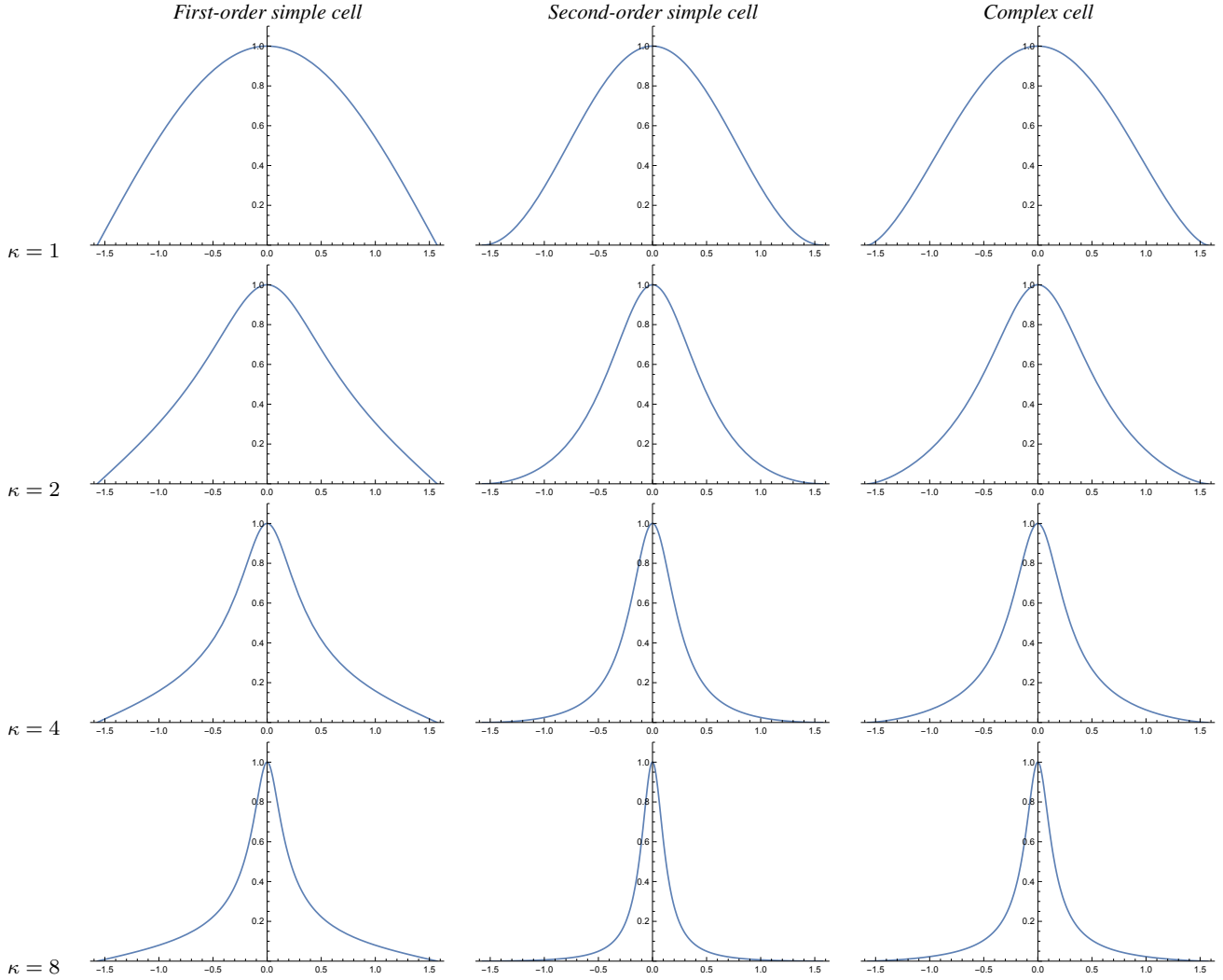


Fig. 2 Graphs of the orientation selectivity for *purely spatial models* of (left column) simple cells in terms of first-order directional derivatives of affine Gaussian kernels, (middle column) simple cells in terms of second-order directional derivatives of affine Gaussian kernels and (right column) complex cells in terms of directional quasi quadrature measures that combine the first- and second-order simple cell responses in a Euclidean way for $C = 1/\sqrt{2}$, and shown for different values of the ratio κ between the spatial scale parameters in the vertical *vs.* the horizontal directions. Observe how the degree of directional selectivity varies strongly depending on the eccentricity $\epsilon = 1/\kappa$ of the receptive fields. (top row) Results for $\kappa = 1$. (second row) Results for $\kappa = 2$. (third row) Results for $\kappa = 4$. (bottom row) Results for $\kappa = 8$. (Horizontal axes: orientation $\theta \in [-\pi/2, \pi/2]$. Vertical axes: Amplitude of the receptive field response.)

$$\mathcal{Q}_{0,spat,norm}L = \sqrt[4]{2}e^{-\frac{1}{\sqrt{2}}} \frac{|\cos \theta|}{\cos^2 \theta + \kappa^2 \sin^2 \theta} \sqrt{\cos^2 \theta + \kappa^2 \sin^2 \theta \cos^2 \left(\frac{\sqrt[4]{2}}{\sqrt{\cos^2 \theta + \kappa^2 \sin^2 \theta}} \left(\frac{x_1 \cos \theta}{\sigma_1} + \frac{x_2 \sin \theta}{\sigma_1} \right) + \beta \right)} \quad (20)$$

Fig. 3 The expression for the oriented spatial quasi quadrature measure $\mathcal{Q}_{0,spat,norm}L$ in the purely spatial model (33) of a complex cell, when applied to a sine wave pattern of the form (21), for $\omega = \omega_Q$ according to (34).

(24)

If we assume that the receptive field is fixed, then the amplitude of the response will depend strongly on the angular frequency ω of the sine wave. The value first increases because of the factor ω and then decreases because of the exponential decrease with ω^2 .

If we assume that a biological experiment regarding orientation selectivity is carried out in such a way that the angular frequency is varied for each inclination angle θ , and then that the result is for each value of θ reported for the angular frequency $\hat{\omega}$ that leads to the maximum response, then we can determine this value of $\hat{\omega}$ by differentiating $A_\varphi(\theta, \omega; \sigma_1, \sigma_2)$ with respect to ω and setting the derivative to zero, which gives:

$$\hat{\omega}_\varphi = \frac{1}{\sigma_1 \sqrt{\cos^2 \theta + \kappa \sin^2 \theta}}, \quad (25)$$

Inserting this values into $A_\varphi(\theta, \omega; \sigma_1, \sigma_2)$, and introducing a scale parameter ratio κ such that

$$\sigma_2 = \kappa \sigma_1, \quad (26)$$

then gives the following orientation selectivity measure

$$A_{\varphi, \max}(\theta, \kappa) = \frac{|\cos \theta|}{\sqrt{e} \sqrt{\cos^2 \theta + \kappa^2 \sin^2 \theta}}. \quad (27)$$

Note, specifically, that this amplitude measure is independent of the spatial scale parameter σ_1 of the receptive field, which, in turn, is a consequence of the scale-invariant nature of differential expressions in terms of scale-normalized derivatives for scale normalization parameter $\gamma = 1$.

The left column in Figure 2 shows the result of plotting the measure $A_{\varphi, \max}(\theta; \kappa)$ of the orientation selectivity as function of the inclination angle θ for a few values of the scale parameter ratio κ , with the values rescaled such that the peak value for each graph is equal to 1. As can be seen from the graphs, the degree of orientation selectivity increases strongly with the value of the spatial scale ratio parameter κ .

3.1.2 Second-order simple cell

Consider next a simple cell that can be modelled as a second-order scale-normalized derivative of an affine Gaussian kernel (according to (1) for $m = 2$), and oriented in the horizontal x_1 -direction (for $\varphi = 0$) with spatial scale parameter σ_1 in the horizontal x_1 -direction and spatial scale parameter σ_2 in the vertical x_2 -direction, and thus again with a spatial covariance matrix of the form $\Sigma_0 = \text{diag}(\sigma_1^2, \sigma_2^2)$:

$$\begin{aligned} T_{00, \text{norm}}(x_1, x_2; \sigma_1, \sigma_2) &= \\ &= \frac{\sigma_1^2}{2\pi\sigma_1\sigma_2} \partial_{x_1 x_1} \left(e^{-x_1^2/2\sigma_1^2 - x_2^2/2\sigma_2^2} \right) \\ &= \frac{(x_1^2 - \sigma_1^2)}{2\pi\sigma_1^3\sigma_2} e^{-x_1^2/2\sigma_1^2 - x_2^2/2\sigma_2^2}. \end{aligned} \quad (28)$$

The corresponding receptive field response is then, again after solving the convolution integral in Mathematica,

$$\begin{aligned} L_{00, \text{norm}}(x_1, x_2; \sigma_1, \sigma_2) &= \\ &= \int_{\xi_1=-\infty}^{\infty} \int_{\xi_2=-\infty}^{\infty} T_{00, \text{norm}}(\xi_1, \xi_2; \sigma_1, \sigma_2) \\ &\quad \times f(x_1 - \xi_1, x_2 - \xi_2) d\xi_1 \xi_2 \\ &= -\omega^2 \sigma_1^2 \cos^2 \theta e^{-\frac{1}{2}\omega^2(\sigma_1^2 \cos^2 \theta + \sigma_2^2 \sin^2 \theta)} \\ &\quad \times \sin(\omega \cos \theta x_1 + \omega \sin \theta x_2 + \beta), \end{aligned} \quad (29)$$

i.e., a sine wave with amplitude

$$A_{\varphi\varphi}(\theta, \omega; \sigma_1, \sigma_2) = \omega^2 \sigma_1^2 \cos^2 \theta e^{-\frac{1}{2}\omega^2(\sigma_1^2 \cos^2 \theta + \sigma_2^2 \sin^2 \theta)}. \quad (30)$$

Again, also this expression first increases and then increases with the angular frequency ω . Selecting again the value of $\hat{\omega}$ at which the amplitude receptive field response assumes its maximum over ω gives

$$\hat{\omega}_{\varphi\varphi} = \frac{\sqrt{2}}{\sigma_1 \sqrt{\cos^2 \theta + \kappa \sin^2 \theta}}, \quad (31)$$

and implies that the maximum amplitude over spatial scales as function of the inclination angle θ and the scale parameter ratio κ can be written

$$A_{\varphi\varphi, \max}(\theta; \kappa) = \frac{\cos^2 \theta}{\sqrt{e} (\cos^2 \theta + \kappa^2 \sin^2 \theta)}. \quad (32)$$

Again, this amplitude measure is also independent of the spatial scale parameter σ_1 of the receptive field, because of the scale-invariant property of scale-normalized derivatives when the scale normalization parameter γ is chosen as $\gamma = 1$.

The middle column in Figure 2 shows the result of plotting the measure $A_{\varphi\varphi, \max}(\theta; \kappa)$ of the orientation selectivity as function of the inclination angle θ for a few values of the scale parameter ratio κ , with the values rescaled such that the peak value for each graph is equal to 1. Again, the degree of orientation selectivity increases strongly with the value of κ , as for the first-order model of a simple cell.

3.1.3 Complex cell

To model the spatial response of a complex cell according to the spatial quasi quadrature measure (4), we combine the responses of the first- and second-order simple cells for $\Gamma = 0$:

$$Q_{0, \text{spat}, \text{norm}} L = \sqrt{L_{00, \text{norm}}^2 + C_\varphi L_{00, \text{norm}}^2}, \quad (33)$$

with $L_{00, \text{norm}}$ according to (23) and $L_{00, \text{norm}}$ according to (29). Choosing the angular frequency $\hat{\omega}$ as the geometric

average of the angular frequencies for which the first- and second-order components of this entity assume their maxima over angular frequencies, respectively,

$$\hat{\omega}_{\mathcal{Q}} = \sqrt{\hat{\omega}_{\varphi} \hat{\omega}_{\varphi\varphi}} = \frac{\sqrt[4]{2}}{\sigma_1 \sqrt{\cos^2 \theta + \kappa^2 \sin^2 \theta}}, \quad (34)$$

with $\hat{\omega}_{\varphi}$ according to (25) and $\hat{\omega}_{\varphi\varphi}$ according to (31). Again letting $\sigma_1 = \kappa \sigma_1$, and setting⁵ the relative weight between first- and second-order information to $C_{\varphi} = 1/\sqrt{2}$ according to (Lindeberg 2018), gives the expression according to Equation (20) in Figure 3.

For inclination angle $\theta = 0$, that measure is spatially constant, in agreement with previous work on closely related isotropic purely spatial isotropic quasi quadrature measures (Lindeberg 2018). Then, the spatial phase dependency increases with increasing values of the inclination angle θ . To select a single representative of those differing representations, let us choose the geometric average of the extreme values, which then assumes the form

$$A_{\mathcal{Q},\text{spat}}(\theta; \kappa) = \frac{\sqrt[4]{2} |\cos \theta|^3}{\sqrt{e} (\cos^2 \theta + \kappa^2 \sin^2 \theta)^{3/4}}. \quad (35)$$

The right column in Figure 2 shows the result of plotting the measure $A_{\mathcal{Q},\text{spat}}(\theta; \kappa)$ of the orientation selectivity as function of the inclination angle θ for a few values of the scale parameter ratio κ , with the values rescaled such that the peak value for each graph is equal to 1. As can be seen from the graphs, the degree of orientation selectivity increases strongly with the value of κ also for this model of a complex cell, and in a qualitatively similar way as for the simple cell models.

3.2 Analysis for space-time separable models of spatio-temporal receptive fields

To investigate the directional selectivity of our spatio-temporal models for simple and complex cells, we will analyze their

⁵ Concerning the choice of the weighting factor C_{φ} between first- and second-order information, it holds that $C_{\varphi} = 1/\sqrt{2}$ implies that the spatial quasi quadrature measure will assume a constant value (be phase independent) for a sine wave at the scale level that is the geometric average of the scale levels at which the scale-normalized amplitudes of the first- and the second-order components in the quasi quadrature measure assume their maxima over scale, for the specific choice of $\gamma = 1$ and $\Gamma = 0$. We will later see manifestations of this property, in that the responses of the different quasi quadrature measures, that we use for modelling complex cells, will be phase independent for inclination angle $\theta = 0$, for an angular frequency that is the geometric average of the angular frequencies for which the first- and second-order components in the quasi quadrature measures will assume their maximum amplitude over scales (see Equations (20), (65) and (66)).

response properties to a moving sine wave of the form

$$\begin{aligned} f(x_1, x_2, t) &= \\ &= \sin(\omega \cos \theta (x_1 - u_1 t) + \omega \sin \theta (x_2 - u_2 t) + \beta), \end{aligned} \quad (36)$$

where we choose the velocity vector $(u_1, u_2)^T$ parallel to the inclination angle θ of the grating according to $(u_1, u_2)^T = (u \cos \theta, u \sin \theta)^T$, which, in turn, implies the form

$$\begin{aligned} f(x_1, x_2, t) &= \\ &= \sin(\omega \cos \theta x_1 + \omega \sin \theta x_2 - u t + \beta). \end{aligned} \quad (37)$$

Let us initially perform such an analysis for space-time separable models of simple and complex cells, in which the velocity vector v in the spatio-temporal receptive field models is set to zero.

For simplicity, we initially perform the theoretical analysis for non-causal spatio-temporal receptive field models, where the temporal components are given as scale-normalized temporal derivatives of 1-D temporal Gaussian kernels.

In the following, we will name our models of spatio-temporal receptive fields according to the orders of differentiation with respect to space and time.

3.2.1 First-order first-order simple cell

Consider a space-time separable receptive field corresponding to a *first-order* scale-normalized Gaussian derivative with scale parameter σ_1 in the horizontal x_1 -direction, a zero-order Gaussian kernel with scale parameter σ_2 in the vertical x_2 -direction, and a *first-order* scale-normalized Gaussian derivative with scale parameter σ_t in the temporal direction, corresponding to $\varphi = 0$, $v = 0$, $\Sigma_0 = \text{diag}(\sigma_1^2, \sigma_2^2)$, $m = 1$ and $n = 1$ in (7):

$$\begin{aligned} T_{0,t,\text{norm}}(x_1, x_2, t; \sigma_1, \sigma_2, \sigma_t) &= \\ &= \frac{\sigma_1 \sigma_t}{(2\pi)^{3/2} \sigma_1 \sigma_2 \sigma_t} \partial_{x_1} \partial_t \left(e^{-x_1^2/2\sigma_1^2 - x_2^2/2\sigma_2^2 - t^2/2\sigma_t^2} \right) \\ &= \frac{x_1 t}{(2\pi)^{3/2} \sigma_1^2 \sigma_2 \sigma_t^2} e^{-x_1^2/2\sigma_1^2 - x_2^2/2\sigma_2^2 - t^2/2\sigma_t^2}. \end{aligned} \quad (38)$$

The corresponding receptive field response is then, after solving the convolution integral in Mathematica,

$$\begin{aligned} L_{0,t,\text{norm}}(x_1, x_2, t; \sigma_1, \sigma_2, \sigma_t) &= \\ &= \int_{\xi_1=-\infty}^{\infty} \int_{\xi_2=-\infty}^{\infty} \int_{\zeta=-\infty}^{\infty} T_{0,t,\text{norm}}(\xi_1, \xi_2, \zeta; \sigma_1, \sigma_2, \sigma_t) \\ &\quad \times f(x_1 - \xi_1, x_2 - \xi_2, t - \zeta) d\xi_1 \xi_2 d\zeta \\ &= \omega^2 \sigma_1 \sigma_t u \cos \theta e^{-\frac{1}{2} \omega^2 (\sigma_1^2 \cos^2 \theta + \sigma_2^2 \sin^2 \theta + \sigma_t^2 u^2)} \\ &\quad \times \sin(\omega \cos \theta x_1 + \omega \sin \theta x_2 - u t + \beta), \end{aligned} \quad (39)$$

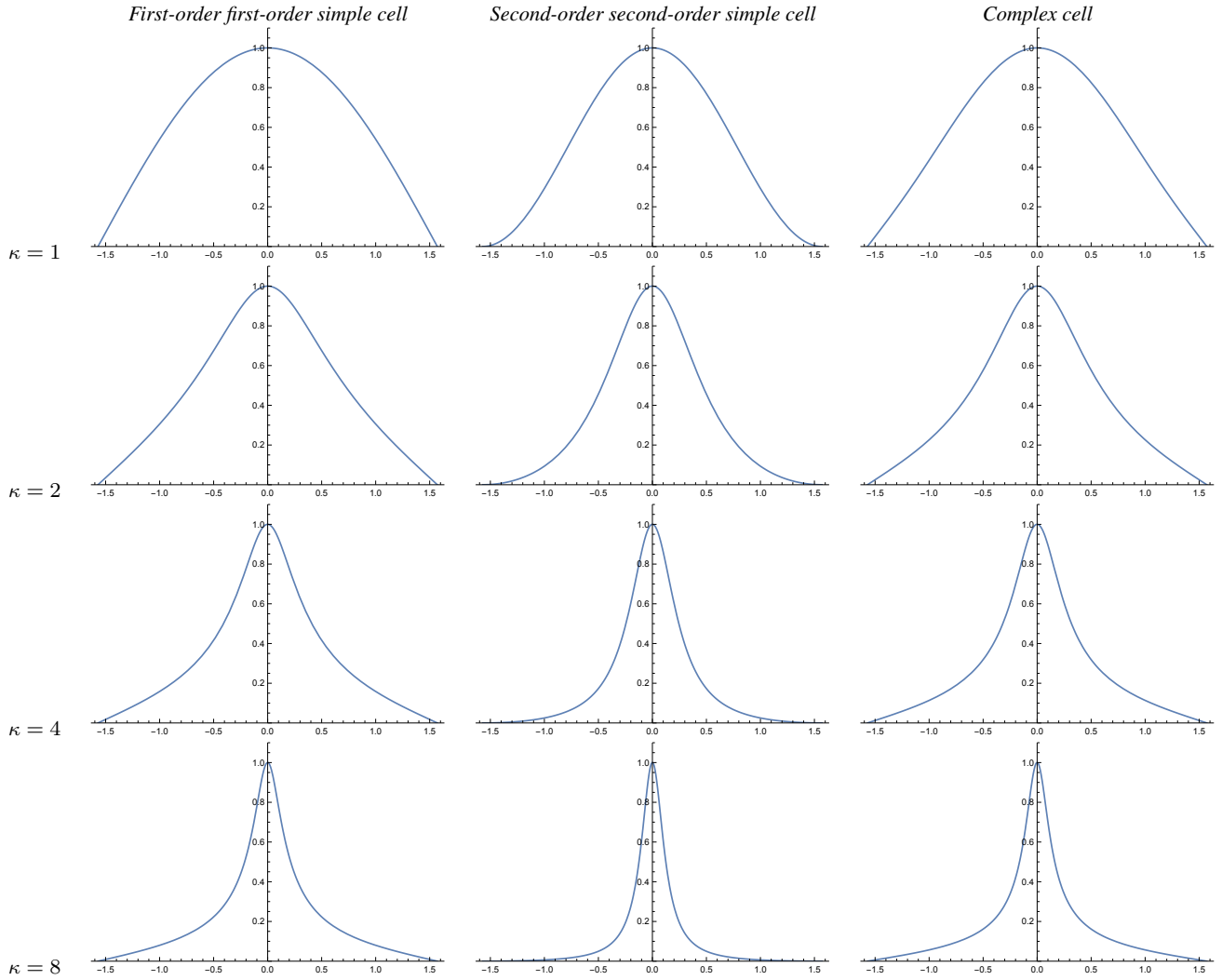


Fig. 4 Graphs of the orientation selectivity for *space-time separable spatio-temporal models* of (left column) simple cells in terms of first-order directional derivatives of affine Gaussian kernels combined with first-order temporal derivatives of temporal Gaussian kernels, (middle column) simple cells in terms of second-order directional derivatives of affine Gaussian kernels combined with second-order temporal derivatives of temporal Gaussian kernels and (right column) complex cells in terms of directional quasi quadrature measures that combine the first- and second-order simple cell responses in a Euclidean way for $C_\varphi = 1/\sqrt{2}$, and $C_t = 1/\sqrt{2}$ shown for different values of the ratio κ between the spatial scale parameters in the vertical *vs.* the horizontal directions. Observe how the degree of directional selectivity varies strongly depending on the eccentricity $\epsilon = 1/\kappa$ of the receptive fields. (top row) Results for $\kappa = 1$. (second row) Results for $\kappa = 2$. (third row) Results for $\kappa = 4$. (bottom row) Results for $\kappa = 8$. (Horizontal axes: orientation $\theta \in [-\pi/2, \pi/2]$. Vertical axes: Amplitude of the receptive field response.)

i.e., a sine wave with amplitude

$$A_{\varphi,t}(\theta, u, \omega; \sigma_1, \sigma_2, \sigma_t) = \omega^2 \sigma_1 \sigma_t u \cos \theta e^{-\frac{1}{2} \omega^2 (\sigma_1^2 \cos^2 \theta + \sigma_2^2 \sin^2 \theta + \sigma_t^2 u^2)}. \quad (40)$$

This expression first increases and then decreases with respect to both the angular frequency ω and velocity u of the sine wave. Selecting the values of $\hat{\omega}$ and \hat{u} at which this expression assumes its maximum over ω and u

$$\hat{\omega}_{\varphi,t} = \frac{1}{\sigma_1 \sqrt{\cos^2 \theta + \kappa \sin^2 \theta}}, \quad (41)$$

$$\hat{u}_{\varphi,t} = \frac{\sigma_1}{\sigma_t} \sqrt{\cos^2 \theta + \kappa \sin^2 \theta}, \quad (42)$$

and again reparameterizing the other spatial scale parameter σ_2 as $\sigma_2 = \kappa \sigma_1$, gives that the maximum amplitude measure over spatial and temporal scales is

$$A_{\varphi,t,\max}(\theta; \kappa) = \frac{\cos \theta}{e \sqrt{\cos^2 \theta + \kappa^2 \sin^2 \theta}}. \quad (43)$$

Note that again this directional selectivity measure is independent of the spatial scale parameter σ_1 as well as independent of the temporal scale parameter σ_t , because of the

scale-invariant property of scale-normalized derivatives for scale normalization power $\gamma = 1$.

The left column in Figure 4 shows the result of plotting the measure $A_{\varphi,t,max}(\theta; \kappa)$ of the orientation selectivity as function of the inclination angle θ for a few values of the scale parameter ratio κ , with the values rescaled such that the peak value for each graph is equal to 1. As we can see from the graphs, as for the previous purely spatial model of the receptive fields, the degree of orientation selectivity increases strongly with the value of κ .

3.2.2 First-order second-order simple cell

Consider a space-time separable receptive field corresponding to a *first-order* scale-normalized Gaussian derivative with scale parameter σ_1 in the horizontal x_1 -direction, a zero-order Gaussian kernel with scale parameter σ_2 in the vertical x_2 -direction, and a *second-order* scale-normalized Gaussian derivative with scale parameter σ_t in the temporal direction, corresponding to $\varphi = 0, v = 0, \Sigma_0 = \text{diag}(\sigma_1^2, \sigma_2^2), m = 1$ and $n = 2$ in (7):

$$\begin{aligned} T_{0,tt,norm}(x_1, x_2, t; \sigma_1, \sigma_2, \sigma_t) &= \\ &= \frac{\sigma_1 \sigma_t^2}{(2\pi)^{3/2} \sigma_1 \sigma_2 \sigma_t} \partial_{x_1} \partial_{tt} \left(e^{-x_1^2/2\sigma_1^2 - x_2^2/2\sigma_2^2 - t^2/2\sigma_t^2} \right) \\ &= -\frac{x_1(t^2 - \sigma_t^2)}{(2\pi)^{3/2} \sigma_1^2 \sigma_2 \sigma_t^3} e^{-x_1^2/2\sigma_1^2 - x_2^2/2\sigma_2^2 - t^2/2\sigma_t^2}. \end{aligned} \quad (44)$$

The corresponding receptive field response is then, after solving the convolution integral in Mathematica,

$$\begin{aligned} L_{0,tt,norm}(x_1, x_2, t; \sigma_1, \sigma_2, \sigma_t) &= \\ &= \int_{\xi_1=-\infty}^{\infty} \int_{\xi_2=-\infty}^{\infty} \int_{\zeta=-\infty}^{\infty} T_{0,tt,norm}(\xi_1, \xi_2, \zeta; \sigma_1, \sigma_2, \sigma_t) \\ &\quad \times f(x_1 - \xi_1, x_2 - \xi_2, t - \zeta) d\xi_1 \xi_2 d\zeta \\ &= -\omega^3 \sigma_1 \sigma_t^2 u^2 \cos \theta e^{-\frac{1}{2}\omega^2(\sigma_1^2 \cos^2 \theta + \sigma_2^2 \sin^2 \theta + \sigma_t^2 u^2)} \\ &\quad \times \cos(\omega \cos \theta x_1 + \omega \sin \theta x_2 - u t + \beta), \end{aligned} \quad (45)$$

i.e., a cosine wave with amplitude

$$\begin{aligned} A_{\varphi,tt}(\theta, u, \omega; \sigma_1, \sigma_2, \sigma_t) &= \\ &= \omega^3 \sigma_1 \sigma_t^2 u^2 \cos \theta e^{-\frac{1}{2}\omega^2(\sigma_1^2 \cos^2 \theta + \sigma_2^2 \sin^2 \theta + \sigma_t^2 u^2)}. \end{aligned} \quad (46)$$

This entity assumes its maximum over the angular frequency ω and the image velocity u at

$$\hat{\omega}_{\varphi,tt} = \frac{1}{\sigma_1 \sqrt{\cos^2 \theta + \kappa \sin^2 \theta}}, \quad (47)$$

$$\hat{u}_{\varphi,tt} = \frac{\sqrt{2}\sigma_1}{\sigma_t} \sqrt{\cos^2 \theta + \kappa \sin^2 \theta}, \quad (48)$$

and again reparameterizing the other spatial scale parameter σ_2 as $\sigma_2 = \kappa \sigma_1$, gives that the maximum amplitude measure over spatial and temporal scales is

$$A_{\varphi,tt,max}(\theta; \kappa) = \frac{2 \cos \theta}{e^{3/2} \sqrt{\cos^2 \theta + \kappa^2 \sin^2 \theta}}, \quad (49)$$

i.e., of a similar form as the previous measure $A_{\varphi,tt,max}(\theta; \kappa)$, while being multiplied by another constant.

3.2.3 Second-order first-order simple cell

Consider a space-time separable receptive field corresponding to a *second-order* scale-normalized Gaussian derivative with scale parameter σ_1 in the horizontal x_1 -direction, a zero-order Gaussian kernel with scale parameter σ_2 in the vertical x_2 -direction, and a *first-order* scale-normalized Gaussian derivative with scale parameter σ_t in the temporal direction, corresponding to $\varphi = 0, v = 0, \Sigma_0 = \text{diag}(\sigma_1^2, \sigma_2^2), m = 2$ and $n = 1$ in (7):

$$\begin{aligned} T_{00,t,norm}(x_1, x_2, t; \sigma_1, \sigma_2, \sigma_t) &= \\ &= \frac{\sigma_1^2 \sigma_t}{(2\pi)^{3/2} \sigma_1 \sigma_2 \sigma_t} \partial_{x_1 x_1} \partial_t \left(e^{-x_1^2/2\sigma_1^2 - x_2^2/2\sigma_2^2 - t^2/2\sigma_t^2} \right) \\ &= -\frac{(x_1^2 - \sigma_1^2)t}{(2\pi)^{3/2} \sigma_1^3 \sigma_2 \sigma_t^2} e^{-x_1^2/2\sigma_1^2 - x_2^2/2\sigma_2^2 - t^2/2\sigma_t^2}. \end{aligned} \quad (50)$$

The corresponding receptive field response is then, after solving the convolution integral in Mathematica,

$$\begin{aligned} L_{00,t,norm}(x_1, x_2, t; \sigma_1, \sigma_2, \sigma_t) &= \\ &= \int_{\xi_1=-\infty}^{\infty} \int_{\xi_2=-\infty}^{\infty} \int_{\zeta=-\infty}^{\infty} T_{00,t,norm}(\xi_1, \xi_2, \zeta; \sigma_1, \sigma_2, \sigma_t) \\ &\quad \times f(x_1 - \xi_1, x_2 - \xi_2, t - \zeta) d\xi_1 \xi_2 d\zeta \\ &= -\omega^3 \sigma_1^2 \sigma_t u \cos^2 \theta e^{-\frac{1}{2}\omega^2(\sigma_1^2 \cos^2 \theta + \sigma_2^2 \sin^2 \theta + \sigma_t^2 u^2)} \\ &\quad \times \cos(\omega \cos \theta x_1 + \omega \sin \theta x_2 - u t + \beta), \end{aligned} \quad (51)$$

i.e., a cosine wave with amplitude

$$\begin{aligned} A_{\varphi\varphi,t}(\theta, u, \omega; \sigma_1, \sigma_2, \sigma_t) &= \\ &= \omega^3 \sigma_1^2 \sigma_t u \cos^2 \theta e^{-\frac{1}{2}\omega^2(\sigma_1^2 \cos^2 \theta + \sigma_2^2 \sin^2 \theta + \sigma_t^2 u^2)}. \end{aligned} \quad (52)$$

This entity assumes its maximum over spatial scale σ_1 and over temporal scale σ_t at

$$\hat{\omega}_{\varphi\varphi,t} = \frac{\sqrt{2}}{\sigma_1 \sqrt{\cos^2 \theta + \kappa \sin^2 \theta}}, \quad (53)$$

$$\hat{u}_{\varphi\varphi,t} = \frac{\sigma_1}{\sqrt{2}\sigma_t} \sqrt{\cos^2 \theta + \kappa \sin^2 \theta}, \quad (54)$$

and again reparameterizing the other spatial scale parameter σ_2 as $\sigma_2 = \kappa \sigma_1$, gives that the maximum amplitude measure over spatial and temporal scales is

$$A_{\varphi\varphi,t,max}(\theta; \kappa) = \frac{2 \cos^2 \theta}{e^{3/2} (\cos^2 \theta + \kappa^2 \sin^2 \theta)}. \quad (55)$$

3.2.4 Second-order second-order simple cell

Consider a space-time separable receptive field corresponding to a *second-order* scale-normalized Gaussian derivative with scale parameter σ_1 in the horizontal x_1 -direction, a zero-order Gaussian kernel with scale parameter σ_2 in the vertical x_2 -direction, and a *second-order* scale-normalized Gaussian derivative with scale parameter σ_t in the temporal direction, corresponding to $\varphi = 0, v = 0, \Sigma_0 = \text{diag}(\sigma_1^2, \sigma_2^2), m = 2$ and $n = 2$ in (7):

$$\begin{aligned} T_{00,tt,norm}(x_1, x_2, t; \sigma_1, \sigma_2, \sigma_t) &= \\ &= \frac{\sigma_1^2 \sigma_t^2}{(2\pi)^{3/2} \sigma_1 \sigma_2 \sigma_t} \partial_{x_1 x_1} \partial_{tt} \left(e^{-x_1^2/2\sigma_1^2 - x_2^2/2\sigma_2^2 - t^2/2\sigma_t^2} \right) \\ &= \frac{(x_1^2 - \sigma_1^2)(t^2 - \sigma_t^2)}{(2\pi)^{3/2} \sigma_1^3 \sigma_2 \sigma_t^3} e^{-x_1^2/2\sigma_1^2 - x_2^2/2\sigma_2^2 - t^2/2\sigma_t^2}. \end{aligned} \quad (56)$$

The corresponding receptive field response is then, after solving the convolution integral in Mathematica,

$$\begin{aligned} L_{00,tt,norm}(x_1, x_2, t; \sigma_1, \sigma_2, \sigma_t) &= \\ &= \int_{\xi_1=-\infty}^{\infty} \int_{\xi_2=-\infty}^{\infty} \int_{\zeta=-\infty}^{\infty} T_{00,tt,norm}(\xi_1, \xi_2, \zeta; \sigma_1, \sigma_2, \sigma_t) \\ &\quad \times f(x_1 - \xi_1, x_2 - \xi_2, t - \zeta) d\xi_1 \xi_2 d\zeta \\ &= \omega^4 \sigma_1^2 \sigma_t^2 u^2 \cos^2 \theta e^{-\frac{1}{2}\omega^2(\sigma_1^2 \cos^2 \theta + \sigma_2^2 \sin^2 \theta + \sigma_t^2 u^2)} \\ &\quad \times \sin(\omega \cos \theta x_1 + \omega \sin \theta x_2 - u t + \beta), \end{aligned} \quad (57)$$

i.e., a sine wave with amplitude

$$\begin{aligned} A_{\varphi\varphi,tt}(\theta, u, \omega; \sigma_1, \sigma_2, \sigma_t) &= \\ &= \omega^4 \sigma_1^2 \sigma_t^2 u^2 \cos^2 \theta e^{-\frac{1}{2}\omega^2(\sigma_1^2 \cos^2 \theta + \sigma_2^2 \sin^2 \theta + \sigma_t^2 u^2)}. \end{aligned} \quad (58)$$

This entity assumes its maximum over spatial scale σ_1 and over temporal scale σ_t at

$$\hat{\omega}_{\varphi\varphi,tt} = \frac{\sqrt{2}}{\sigma_1 \sqrt{\cos^2 \theta + \kappa \sin^2 \theta}}, \quad (59)$$

$$\hat{u}_{\varphi\varphi,tt} = \frac{\sigma_1}{\sigma_t} \sqrt{\cos^2 \theta + \kappa \sin^2 \theta}, \quad (60)$$

and again reparameterizing the other spatial scale parameter σ_2 as $\sigma_2 = \kappa \sigma_1$, gives that the maximum amplitude measure over spatial and temporal scales is

$$A_{\varphi\varphi,tt,max}(\theta; \kappa) = \frac{4 \cos^2 \theta}{e^2 (\cos^2 \theta + \kappa^2 \sin^2 \theta)}. \quad (61)$$

The middle column in Figure 4 shows the result of plotting the measure $A_{\varphi\varphi,tt,max}(\theta; \kappa)$ of the orientation selectivity as function of the inclination angle θ for a few values of the scale parameter ratio κ , with the values rescaled such that the peak value is equal to 1. Again, the degree of orientation selectivity increases strongly with the value of κ , as for the first-order first-order model of a simple cell.

3.2.5 Complex cell

To model the spatio-temporal response of a complex cell according to the directional sensitive spatio-temporal quasi quadrature measure (7) based on space-time separable spatio-temporal receptive fields, we combine the responses of the first-order first-order simple cell (39), the first-order second-order cell (45), the second-order first-order simple cell (51) and the second-order second order cell (57) for $v = 0, \Gamma_\varphi = 0$ and $\Gamma_t = 0$ according to

$$\begin{aligned} &(\mathcal{Q}_{0,sep,norm} L)^2 \\ &= L_{0,t,norm}^2 + C_\varphi L_{00,t,norm}^2 + \\ &\quad + C_t (L_{0,tt,norm}^2 + C_\varphi L_{00,tt,norm}^2). \end{aligned} \quad (62)$$

Selecting the angular frequency $\hat{\omega}$ as the geometric average of the angular frequencies where the above spatio-temporal simple cell models assume their maximum amplitude responses over spatial scales

$$\hat{\omega}_Q = \sqrt{\hat{\omega}_{\varphi,t} \hat{\omega}_{\varphi,tt} \hat{\omega}_{\varphi\varphi,t} \hat{\omega}_{\varphi\varphi,tt}} = \frac{\sqrt{2}}{\sigma_1 \sqrt{\cos^2 \theta + \kappa \sin^2 \theta}}, \quad (63)$$

and selecting the image velocity \hat{u} of the sine wave as the geometric average of the image velocities where the above spatio-temporal simple cell models assume their maximum amplitude responses over image velocities

$$\hat{u}_Q = \sqrt{\hat{u}_{\varphi,t} \hat{u}_{\varphi,tt} \hat{u}_{\varphi\varphi,t} \hat{u}_{\varphi\varphi,tt}} = \frac{\sigma_1}{\sigma_t} \sqrt{\cos^2 \theta + \kappa \sin^2 \theta}, \quad (64)$$

as well as choosing the spatial and temporal weighting factors C_φ and C_t between first- and second-order information as $C_\varphi = 1/\sqrt{2}$ and $C_t = 1/\sqrt{2}$ according to (Lindeberg 2018), then implies that the spatio-temporal quasi quadrature measure assumes the form

$$A_{Q,sep}(\theta; \kappa) = \frac{e^{-\sqrt{2} |\cos \theta| \sqrt{2 + \kappa^2 + (2 - \kappa^2) \cos 2\theta}}}{\cos^2 \theta + \kappa^2 \sin^2 \theta}. \quad (65)$$

Note that this expression is independent of both the spatial scale parameter σ_1 and the temporal scale parameter σ_t , because of the scale-invariant properties of scale-normalized derivatives for scale normalization parameter $\gamma = 1$. Moreover, this expression is also independent of the phase of the signal, as determined by the spatial coordinates x_1 and x_2 , the time moment t and the phase angle β .

The right column in Figure 4 shows the result of plotting the measure $A_{Q,sep}(\theta; \kappa)$ of the orientation selectivity as function of the inclination angle θ for a few values of the scale parameter ratio κ , with the values rescaled such that the peak value for each graph is equal to 1. As can be

seen from the graphs, the degree of orientation selectivity increases strongly with the value of κ also for this spatio-temporal model of a complex cell, and in a qualitatively similar way as for the simple cell models, regarding both the purely spatial as well as the joint spatio-temporal models of the simple cells.

3.3 Analysis for velocity-adapted spatio-temporal models of receptive fields

Similar to previous section, we will again analyze the response properties of spatio-temporal receptive fields to a moving sine wave of the form (37)

$$f(x_1, x_2, t) = \sin(\omega \cos \theta x_1 + \omega \sin \theta x_2 - ut + \beta). \quad (67)$$

Based on the observation that the response properties of temporal derivatives will be zero, if the velocity v of the spatio-temporal receptive field is adapted to the velocity u of the moving sine wave, we will study the case when the temporal order of differentiation n is zero.

3.3.1 First-order simple cell

Consider a velocity-adapted receptive field corresponding to a *first-order* scale-normalized Gaussian derivative with scale parameter σ_1 and velocity v in the horizontal x_1 -direction, a zero-order Gaussian kernel with scale parameter σ_2 in the vertical x_2 -direction, and a zero-order Gaussian derivative with scale parameter σ_t in the temporal direction, corresponding to $\varphi = 0$, $v = 0$, $\Sigma_0 = \text{diag}(\sigma_1^2, \sigma_2^2)$, $m = 1$ and $n = 0$ in (7):

$$T_{0,norm}(x_1, x_2, t; \sigma_1, \sigma_2, \sigma_t) = \frac{\sigma_1}{(2\pi)^{3/2} \sigma_1 \sigma_2 \sigma_t} \partial_{x_1} \left(e^{-x_1^2/2\sigma_1^2 - x_2^2/2\sigma_2^2 - t^2/2\sigma_t^2} \right) \Big|_{x_1 \rightarrow x_1 - vt} = \frac{(x_1 - vt)}{(2\pi)^{3/2} \sigma_1^2 \sigma_2 \sigma_t} e^{-(x_1 - vt)^2/2\sigma_1^2 - x_2^2/2\sigma_2^2 - t^2/2\sigma_t^2}. \quad (68)$$

The corresponding receptive field response is then, after solving the convolution integral in Mathematica,

$$L_{0,norm}(x_1, x_2, t; \sigma_1, \sigma_2, \sigma_t) = \int_{\xi_1=-\infty}^{\infty} \int_{\xi_2=-\infty}^{\infty} \int_{\zeta=-\infty}^{\infty} T_{0,norm}(\xi_1, \xi_2, \zeta; \sigma_1, \sigma_2, \sigma_t) \times f(x_1 - \xi_1, x_2 - \xi_2, t - \zeta) d\xi_1 \xi_2 d\zeta = \omega \sigma_1 \cos \theta \times e^{-\frac{\omega^2}{2} ((\sigma_1^2 + \sigma_t^2 v^2) \cos^2 \theta + \sigma_2^2 \sin^2 \theta - 2\sigma_t^2 u v \cos \theta + \sigma_t^2 u^2)} \times \cos(\cos \theta x_1 + \sin \theta x_2 - \omega u t + \beta), \quad (69)$$

i.e., a cosine wave with amplitude

$$A_\varphi(\theta, u, \omega; \sigma_1, \sigma_2, \sigma_t) = \omega \sigma_1 \cos \theta \times e^{-\frac{\omega^2}{2} (\cos^2 \theta (\sigma_1^2 + \sigma_t^2 v^2) + \sigma_2^2 \sin^2 \theta - 2\sigma_t^2 u v \cos \theta + \sigma_t^2 u^2)}. \quad (70)$$

Assume that a biological experiment regarding the response properties of the receptive field is performed by varying both the angular frequency ω and the image velocity u to get the maximum value of the response over these parameters. Differentiating the amplitude A_φ with respect to ω and u and setting these derivative to zero then gives

$$\hat{\omega}_\varphi = \frac{1}{\sigma_1 \sqrt{\cos^2 \theta + \kappa \sin^2 \theta}}, \quad (71)$$

$$\hat{u}_\varphi = v \cos \theta. \quad (72)$$

Inserting these values into $A_\varphi(\theta, u, \omega; \sigma_1, \sigma_2, \sigma_t)$ then gives the following orientation selectivity measure

$$A_{\varphi,max}(\theta, \kappa) = \frac{\cos \theta}{\sqrt{e \sqrt{\cos^2 \theta + \kappa^2 \sin^2 \theta}}}. \quad (73)$$

The left column in Figure 5 shows the result of plotting the measure $A_{\varphi,max}(\theta; \kappa)$ of the orientation selectivity as function of the inclination angle θ for a few values of the scale parameter ratio κ , with the values rescaled such that the peak value for each graph is equal to 1. As we can see from the graphs, as for the previous purely spatial models of the receptive fields, as well as for the previous space-time separable model of the receptive fields, the degree of orientation selectivity increases strongly with the value of κ .

3.3.2 Second-order simple cell

Consider next a velocity-adapted receptive field corresponding to a *second-order* scale-normalized Gaussian derivative with scale parameter σ_1 and velocity v in the horizontal x_1 -direction, a zero-order Gaussian kernel with scale parameter σ_2 in the vertical x_2 -direction, and a zero-order Gaussian derivative with scale parameter σ_t in the temporal direction, corresponding to $\varphi = 0$, $v = 0$, $\Sigma_0 = \text{diag}(\sigma_1^2, \sigma_2^2)$, $m = 2$ and $n = 0$ in (7):

$$T_{00,norm}(x_1, x_2, t; \sigma_1, \sigma_2, \sigma_t) = \frac{\sigma_1^2}{(2\pi)^{3/2} \sigma_1 \sigma_2 \sigma_t} \partial_{x_1 x_1} \left(e^{-x_1^2/2\sigma_1^2 - x_2^2/2\sigma_2^2 - t^2/2\sigma_t^2} \right) \Big|_{x_1 \rightarrow x_1 - vt} = \frac{(x_1 - vt)^2 - \sigma_1^2}{(2\pi)^{3/2} \sigma_1^3 \sigma_2 \sigma_t} e^{-(x_1 - vt)^2/2\sigma_1^2 - x_2^2/2\sigma_2^2 - t^2/2\sigma_t^2}. \quad (74)$$

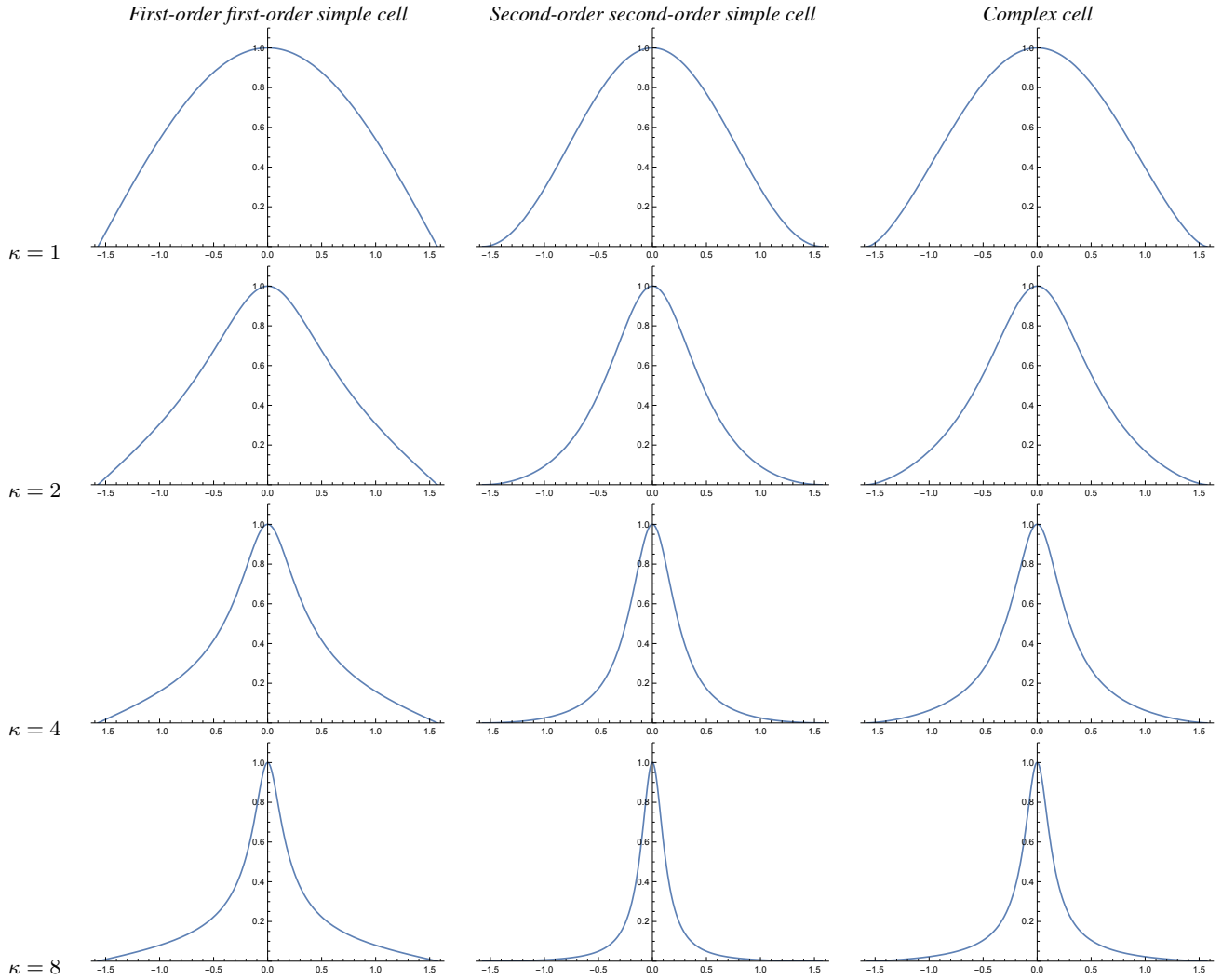


Fig. 5 Graphs of the orientation selectivity for *velocity-adapted spatio-temporal models* of (left column) simple cells in terms of first-order directional derivatives of affine Gaussian kernels combined with zero-order temporal Gaussian kernels, (middle column) simple cells in terms of second-order directional derivatives of affine Gaussian kernels combined with zero-order temporal Gaussian kernels and (right column) complex cells in terms of directional quasi quadrature measures that combine the first- and second-order simple cell responses in a Euclidean way for $C_\varphi = 1/\sqrt{2}$ shown for different values of the ratio κ between the spatial scale parameters in the vertical vs. the horizontal directions. Observe how the degree of directional selectivity varies strongly depending on the eccentricity $\epsilon = 1/\kappa$ of the receptive fields. (top row) Results for $\kappa = 1$. (second row) Results for $\kappa = 2$. (third row) Results for $\kappa = 4$. (bottom row) Results for $\kappa = 8$. (Horizontal axes: orientation $\theta \in [-\pi/2, \pi/2]$. Vertical axes: Amplitude of the receptive field response.)

$$\mathcal{Q}_{0,vel,norm}L = \sqrt[4]{2} e^{-\frac{1}{\sqrt{2}}} \frac{|\cos \theta|}{\cos^2 \theta + \kappa^2 \sin^2 \theta} \sqrt{\cos^2 \theta + \kappa^2 \sin^2 \theta \cos^2 \left(\frac{2^{3/4}(\cos \theta (x_1 - vt) + \sin \theta x_2)}{\sigma_1 \sqrt{1 + \kappa^2 - (\kappa^2 - 1) \cos 2\theta}} + \beta \right)} \quad (66)$$

Fig. 6 The expression for the oriented spatio-temporal quasi quadrature measure $\mathcal{Q}_{0,vel,norm}L$ in the velocity-adapted spatio-temporal model (17) of a complex cell, when applied to a sine wave pattern of the form (67), for $\omega = \omega_Q$ according to (81) and $u = u_Q$ according to (82).

	Purely spatial model	Space-time separable spatio-temporal model	Velocity-adapted spatio-temporal model
First-order simple cell	$\frac{ \cos \theta }{\sqrt{\cos^2 \theta + \kappa^2 \sin^2 \theta}}$	$\frac{ \cos \theta }{\sqrt{\cos^2 \theta + \kappa^2 \sin^2 \theta}}$	$\frac{ \cos \theta }{\sqrt{\cos^2 \theta + \kappa^2 \sin^2 \theta}}$
Second-order simple cell	$\frac{\cos^2 \theta}{\cos^2 \theta + \kappa^2 \sin^2 \theta}$	$\frac{\cos^2 \theta}{\cos^2 \theta + \kappa^2 \sin^2 \theta}$	$\frac{\cos^2 \theta}{\cos^2 \theta + \kappa^2 \sin^2 \theta}$
Complex cell	$\frac{ \cos \theta ^{3/2}}{(\cos^2 \theta + \kappa^2 \sin^2 \theta)^{3/4}}$	$\frac{ \cos \theta \sqrt{2 + \kappa^2 + (2 - \kappa^2) \cos 2\theta}}{\cos^2 \theta + \kappa^2 \sin^2 \theta}$	$\frac{ \cos \theta ^{3/2}}{(\cos^2 \theta + \kappa^2 \sin^2 \theta)^{3/4}}$

Table 1 Summary of the forms of the orientation selectivity functions derived from the theoretical models of simple cells and complex cells based on the generalized Gaussian derivative model for visual receptive fields, in the cases of either (i) purely spatial models, (ii) space-time separable models and (iii) velocity-adapted spatio-temporal models. Concerning the notation, the term “first-order simple cell” means a model of a simple cell corresponding to a first-order directional derivative of an affine Gaussian kernel over the spatial domain, whereas the term “second-order simple cell” means a model of a simple cell corresponding to a second-order directional derivative of an affine Gaussian kernel over the spatial domain. As we can see from the table, the form of the orientation selectivity function is similar for all the models of first-order simple cells. The form of the orientation selectivity function is also similar for all the models of second-order simple cells. For complex cells, the orientation selectivity function of the space-time separable model is, however, different from the orientation selectivity function of the purely spatial model and the velocity-adapted spatio-temporal model, which both have similar orientation selectivity functions. Note, in particular, that common for all these models is the fact that the degree of orientation selectivity increases with the scale parameter ratio $\kappa = \sigma_2/\sigma_1$, which is the ratio between the scale parameter σ_2 in the direction $\perp\varphi$ perpendicular to the preferred orientation φ of the receptive field and the scale parameter σ_1 in the preferred orientation φ of the receptive field.

The corresponding receptive field response is then, after solving the convolution integral in Mathematica,

$$\begin{aligned}
L_{00,norm}(x_1, x_2, t; \sigma_1, \sigma_2, \sigma_t) &= \\
&= \int_{\xi_1=-\infty}^{\infty} \int_{\xi_2=-\infty}^{\infty} \int_{\zeta=-\infty}^{\infty} T_{00,norm}(\xi_1, \xi_2, \zeta; \sigma_1, \sigma_2, \sigma_t) \\
&\quad \times f(x_1 - \xi_1, x_2 - \xi_2, t - \zeta) d\xi_1 \xi_2 d\zeta \\
&= -\omega^2 \sigma_1^2 \cos^2 \theta \\
&\quad \times e^{-\frac{\omega^2}{2} ((\sigma_1^2 + \sigma_t^2 v^2) \cos^2 \theta + \sigma_2^2 \sin^2 \theta - 2\sigma_t^2 uv \cos \theta + \sigma_t^2 u^2)} \\
&\quad \times \cos(\sin \theta x_1 + \sin \theta x_2 - \omega u t + \beta), \quad (75)
\end{aligned}$$

i.e., a sine wave with amplitude

$$\begin{aligned}
A_{\varphi\varphi}(\theta, u, \omega; \sigma_1, \sigma_2, \sigma_t) &= \\
&= \omega^2 \sigma_1^2 \cos^2 \theta \\
&\quad \times e^{-\frac{\omega^2}{2} (\cos^2 \theta (\sigma_1^2 + \sigma_t^2 v^2) + \sigma_2^2 \sin^2 \theta - 2\sigma_t^2 uv \cos \theta + \sigma_t^2 u^2)}. \quad (76)
\end{aligned}$$

Assume that a biological experiment regarding the response properties of the receptive field is performed by varying both the angular frequency ω and the image velocity u to get the maximum value of the response over these parameters. Differentiating the amplitude $A_{\varphi\varphi}$ with respect to ω and u and setting these derivative to zero then gives

$$\hat{\omega}_{\varphi\varphi} = \frac{\sqrt{2}}{\sigma_1 \sqrt{\cos^2 \theta + \kappa \sin^2 \theta}}, \quad (77)$$

$$\hat{u}_{\varphi\varphi} = v \cos \theta. \quad (78)$$

Inserting these values into $A_{\varphi\varphi}(\theta, u, \omega; \sigma_1, \sigma_2, \sigma_t)$ then gives the following orientation selectivity measure

$$A_{\varphi\varphi,max}(\theta, \kappa) = \frac{2 \cos^2 \theta}{e (\cos^2 \theta + \kappa^2 \sin^2 \theta)}. \quad (79)$$

The middle column in Figure 5 shows the result of plotting the measure $A_{\varphi\varphi,max}(\theta; \kappa)$ of the orientation selectivity as function of the inclination angle θ for a few values of the scale parameter ratio κ , with the values rescaled such that the peak value for each graph is equal to 1. Again, the degree of orientation selectivity increases strongly with the value of κ .

3.3.3 Complex cell

To model the spatial response of a complex cell according to the spatio-temporal quasi quadrature measure (17) based on velocity-adapted spatio-temporal receptive fields, we combine the responses of the first- and second-order simple cells (for $\Gamma = 0$)

$$(\mathcal{Q}_{0,vel,norm} L) = \sqrt{\frac{L_{0,norm}^2 + C_\varphi L_{00,norm}^2}{\sigma_\varphi^{2\Gamma}}}, \quad (80)$$

with $L_{0,norm}$ according to (69) and $L_{00,norm}$ according to (75).

Selecting the angular frequency as the geometric average of the angular frequency values at which the above spatio-temporal simple cell models assume their maxima over angular frequencies, as well as using the same value of u ,

$$\hat{\omega}_{\mathcal{Q}} = \sqrt{\hat{\omega}_\varphi \hat{\omega}_{\varphi\varphi}} = \frac{\sqrt[4]{2}}{\sigma_1 \sqrt{\cos^2 \theta + \kappa \sin^2 \theta}}, \quad (81)$$

with $\hat{\omega}_\varphi$ according to (71) and $\hat{\omega}_{\varphi\varphi}$ according to (77), as well as choosing the image velocity \hat{u} as the same value as for which the above spatio-temporal simple cell models assume their maxima over the image velocity ((72) and (78))

$$\hat{u}_{\mathcal{Q}} = v \cos \theta, \quad (82)$$

as well as letting $\sigma_1 = \kappa \sigma_1$, and setting the relative weights between first- and second-order information to $C_\varphi = 1/\sqrt{2}$

and $C_t = 1/\sqrt{2}$ according to (Lindeberg 2018), then gives the expression according to Equation (66) in Figure 6.

For inclination angle $\theta = 0$, that measure is spatially constant, in agreement with our previous purely spatial analysis, as well as in agreement with previous work on closely related isotropic spatio-temporal quasi quadrature measures (Lindeberg 2018). When the inclination angle increases, the phase dependency of the quasi quadrature measure will, however, increase. To select a single representative of those differing representations, let us choose the geometric average of the extreme values, which then assumes the form

$$A_{Q,vel,max}(\theta; \kappa) = \frac{\sqrt[4]{2} |\cos \theta|^{3/2}}{e^{1/\sqrt{2}} (\cos^2 \theta + \kappa^2 \sin^2 \theta)^{3/2}}. \quad (83)$$

The right column in Figure 5 shows the result of plotting the measure $A_{Q,vel,max}(\theta; \kappa)$ of the orientation selectivity as function of the inclination angle θ for a few values of the scale parameter ratio κ , with the values rescaled such that the peak value for each graph is equal to 1. Again, the degree of orientation selectivity increases strongly with the value of κ .

3.4 Resulting models for orientation selectivity

Table 1 summarizes the results from the above theoretical analysis of the orientation selectivity for our idealized models of simple cells and complex cells, based on the generalized Gaussian derivative model for visual receptive fields, in the cases of either (i) purely spatial models, (ii) space-time separable models and (iii) velocity-adapted spatio-temporal models. The overall method that we have used for deriving these results is by exposing each theoretical receptive field model to either purely spatial or joint spatio-temporal sine wave patterns, and measuring the response properties for different inclination angles θ , at the angular frequency of the sine wave, as well as the image velocity of the spatio-temporal sine wave, at which these models assume their maximum response over variations of these testing parameters.

As can be seen from the table, the form of the orientation selectivity curve is similar for all the models of first-order simple cells, which correspond to first-order derivatives of affine Gaussian kernels over the spatial domain. The form of the orientation selectivity curve is also similar for all the models of second-order simple cells, which correspond to second-order derivatives of affine Gaussian kernels over the spatial domain. For complex cells, the form of the orientation selectivity curve for the space-time separable model is, however, different from the form of the orientation selectivity curve for the purely spatial model and the velocity-adapted spatio-temporal model, which both have a similar form for their orientation selectivity curves.

Note, in particular, that common for all these models is the fact that the degree of orientation selectivity increases

with the scale parameter ratio $\kappa = \sigma_2/\sigma_1$, which is the ratio between the scale parameter σ_2 in the direction $\perp \varphi$ perpendicular to the preferred orientation φ of the receptive field and the scale parameter σ_1 in the preferred orientation φ of the receptive field. In other words, for higher values of κ , the form of the orientation selectivity curve is more narrow than the form of the orientation selectivity curve for a lower value of κ . The form of the orientation selectivity curve is also more narrow for a simple cell that can be modelled as a second-order directional derivative of an affine Gaussian kernel, than for a simple cell that can be modelled as a first order derivative of an affine Gaussian kernel.

In this respect, the theoretical analysis supports the conclusion that the degree of orientation selectivity of the receptive fields increases with the degree of anisotropy of the receptive fields, specifically the fact that highly anisotropic affine Gaussian derivative based receptive fields have higher degree of orientation selectivity than more isotropic affine Gaussian derivative based receptive fields.

4 Implications for biological vision

In this section, we will compare the results of the above theoretical predictions with biological results concerning the orientation selectivity of visual neurons.

Nauhaus *et al.* (2008) have measured the orientation tuning of neurons at different positions in the primary visual cortex for monkey and cat. They found that orientation tuning is broader near pinwheel centers and sharper in regions of homogeneous orientation preference. Figure 7 shows an overview of their results, where we can see how the degree of orientation selectivity changes rather continuously from broad to sharp with increasing distance from the pinwheel center (from top to bottom in the figure).

In view of our theoretical results in Section 3, concerning the orientation selectivity of receptive fields, where the spatial smoothing part is performed based on affine Gaussian kernels, this qualitative behaviour is similar to what would be the result if the ratio κ between the two scale parameters of the underlying affine Gaussian kernels, in the idealized models of spatial and spatio-temporal receptive fields in Section 2, would increase from a lower to a higher value, when moving away from the pinwheels on the cortical surface. In this sense, the theoretical predictions from the presented theory are consistent with the results by Nauhaus *et al.*, with the additional explanatory value in that the theoretical predictions also may enable a deeper interpretation of those biological results, in terms of underlying computational mechanisms in the visual receptive fields.

A highly interesting quantitative measurement to perform would hence be to fit parameterized models of the orientation selectivity, according to the summary in Table 1, to

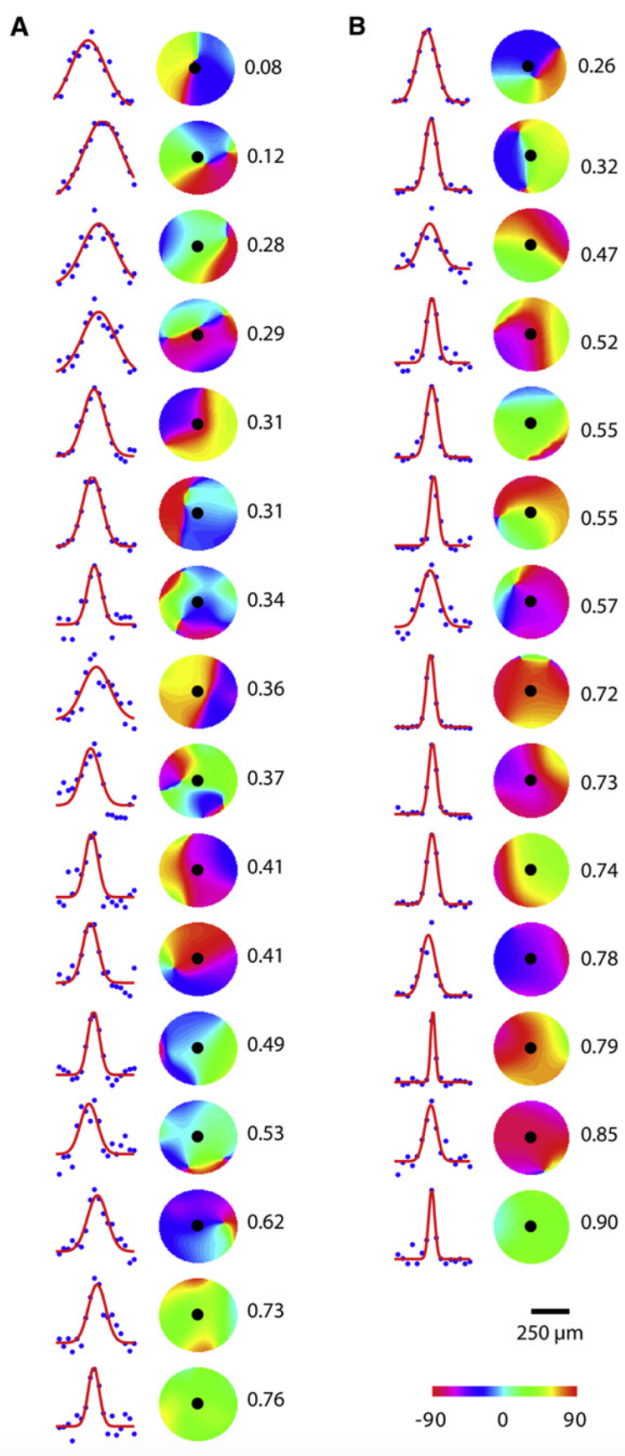


Fig. 7 Measurements of the orientation tuning of neurons, at different positions in the visual cortex, according to Nauhaus *et al.* (2008) (Copyright Cell Press with permission). In this figure it can be seen how the orientation tuning changes from broad to sharp, and thus higher degree of orientation selectivity, with increasing distance from the pinwheels, consistent with the qualitative behaviour that would be obtained if the ratio κ , between the scale parameters in underlying affine Gaussian smoothing step in the idealized models of spatial and spatio-temporal receptive fields, would increase when moving away from the pinwheels on the cortical surface.

orientation tuning curves of the form recorded by Nauhaus *et al.* (2008), to get estimates of the distribution of the parameter κ over a sufficiently large population of visual neurons, under the assumption that the spatial components of the biological receptive fields can be well modelled by affine Gaussian derivatives.⁶

In (Lindeberg 2023), a theoretical treatment is given concerning covariance properties of visual receptive fields under natural image transformations, specifically geometric image transformations in terms of spatial scaling transformations, spatial affine transformations, Galilean transformations and temporal scaling transformations. According to that theory of spatial and spatio-temporal receptive fields in terms of generalized Gaussian derivative based receptive fields, the covariance properties of the receptive fields mean that the shapes of the receptive field families span the degrees of freedom generated by the geometric image transformations. With regard to spatial affine transformations, which beyond spatial scaling transformations do also comprise spatial rotations and non-uniform scaling transformation with different amount of scaling in two orthogonal spatial directions, this theory implies that affine Gaussian kernels should be present in the receptive field families corresponding to different values of the ratio κ between the spatial scale parameters, in order to support affine covariance. In (Lindeberg 2023 Section 3.2) suggestions to new biological measurements were further proposed to support (or reject) those hypotheses.

By combining theoretical predictions in this article with the biological results by Nauhaus *et al.* (2008), we can get indirect support for the hypothesis concerning an expansion of receptive field shapes over variations in the ratio between the two scale parameters of spatially anisotropic receptive fields. If we assume that the biological receptive fields can be well modelled by the generalized Gaussian derivative model based on affine Gaussian receptive fields, then the biological results by Nauhaus *et al.* (2008) are fully consistent with the predictions obtained from the presented theory, concerning the orientation selectivity of visual receptive fields, whose spatial smoothing component can be well modelled by affine Gaussian kernels.

Based on these results we propose that, beyond an expansion over rotations, as is performed in current models of the pinwheel structure of visual receptive fields (Bonhoeffer and Grinvald 1991; Blasdel 1992; Swindale 1996; Petitot 2003; Baspinar *et al.* 2018; Liu and Robinson 2022), also the eccentricity ϵ of the receptive fields (the inverse of the parameter κ) should be taken into account when modelling the pinwheel structure in the visual cortex.

⁶ At the point of writing this article, the author does, however, not have access to the data that would be needed to perform such an analysis.

5 Summary and discussion

We have presented an in-depth theoretical analysis of the orientation selectivity for the spatial and spatio-temporal receptive fields in the generalized Gaussian derivative model for visual receptive fields. This model for visual receptive fields has been previously derived in an axiomatic manner, from symmetry properties of the environment, in combination with requirements of internal consistency between image representations over multiple spatial and temporal scales, and has been demonstrated to well capture the properties of biological simple cells in the primary visual cortex. Building upon that theory for linear receptive fields, we have also analysed the orientation selectivity for non-linear models of complex cells, based on energy models that combine the output from such models for simple cells for different orders of spatial differentiation.

Specifically, we have analyzed how the orientation selectivity depends on a scale parameter ratio κ , between the scale parameters in the image orientations perpendicular to *vs.* parallel with the preferred orientation of the receptive fields. Explicit expressions for the resulting tuning curves have been derived, based on closed form theoretical analysis, and it has been shown that, for all these models of visual receptive fields, the degree of orientation selectivity becomes more narrow with increasing values of the scale parameter ratio κ .

By comparisons with previously established results by Nauhaus *et al.* (2008), we have demonstrated that the predictions from our theory are consistent with general behaviour of visual neurons in the primary visual cortex, in that the orientation tuning is broader near the pinwheels, while the orientation selectivity becomes sharper further away.

By combining these two results, we have also provided indirect support for a previously formulated biological hypothesis in (Lindeberg 2023), stating that the family of receptive field shapes should span the degrees of freedom in the natural geometric image transformations, in the sense that the receptive field shapes should span a sufficiently wide range of ratios between the scale parameters in the directions perpendicular to *vs.* parallel with the preferred orientation of the receptive field, to support affine covariance of the family of visual receptive fields.

Concerning extensions of the approach, we have in the present treatment limited ourselves to receptive fields corresponding to only first- and second-order derivatives over the spatial domain. Modelling results by Young (1987) have, however, demonstrated that receptive fields up to fourth order of spatial differentiation may be present in the primary visual cortex. It is straightforward to extend our analysis to third- and fourth-order directional derivatives, which would then give other closed-form expressions for the orientation selectivity of the receptive fields (and more narrow than the

orientation selectivity for first- and second-order derivatives). Models of complex cells involving third- and fourth-order spatial derivatives could also be formulated and be theoretically analyzed (although experimental support for such extended models of complex cells may currently not be available).

A more conceptual way of extending the modelling work would also be to incorporate a complementary spatial smoothing step in model of complex cells, as used in (Lindeberg 2020 Section 5). In the models for complex cells used in the theoretical analysis in this paper, the responses of first- and second-order spatial derivative based receptive fields have been throughout combined in a pointwise manner, over both space and time. A more general approach would, however, be to perform weighted integration of such pointwise contributions over a wider support region over space and time, with the size over the spatial image domain and the duration over the temporal domain proportional to the local spatial and temporal scales at which the spatial and temporal derivatives are computed. In the present treatment, we have, however, not extended the complex cell models in that way, although it could be well motivated, mainly to simplify the treatment, and to limit the complexity of the theoretical analysis.

Concerning the spatio-temporal models of the receptive fields, we have also limited ourselves to performing a non-causal temporal analysis, where the temporal smoothing kernels are 1-D Gaussian kernels. To perform a corresponding time-causal temporal analysis, based on using the time-causal limit kernel for temporal smoothing, one can perform a Fourier analysis to determine how the probing sine wave will be affected, using the closed-form expression for the Fourier transform of the time-causal limit kernel, in a similar way as in the temporal scale selection analysis in (Lindeberg 2017 Section 5.2).

Concerning the way that the orientation selectivity curves are defined, we have in the above theoretical analysis throughout assumed that the wavelength $\hat{\omega}$ (and for the spatio-temporal analysis also the image velocity \hat{u}) of the probing sine wave is optimized for each image orientation separately. Another possibility is to instead assume that the wavelength is only optimized for the preferred orientation of the receptive field, and then held constant for all the other image orientations. Changing the probing method in such a way would change the shapes of the orientation selectivity curves, but can be easily performed, based on the principles for theoretical analysis outlined in the above treatment.

One could possibly also consider extending the analysis to different values of the scale normalization powers γ and Γ , than using the maximally scale invariant choices $\gamma = 1$ and $\Gamma = 0$ used for simplicity in this treatment. Then, however, some type of post-normalization may, however, also be necessary, to make it possible to appropriately compare re-

ceptive field responses between multiple spatial and temporal scales, which otherwise are perfectly comparable when using $\gamma = 1$ and $\Gamma = 0$.

Concerning possible limitations of the approach, it should be emphasized that the models for visual receptive fields in the generalized Gaussian derivative model are highly idealized. They have been derived from mathematical analysis based on idealized theoretical assumptions, regarding symmetry properties of the environment, while have not been quantitatively adjusted to the receptive field shapes of actual biological neurons. Hence, the results from the presented theoretical analysis should be interpreted as such, as the results of a maximally idealized model, and not with specific aims of providing a numerically accurate representation of actual biological neurons. The receptive field models also constitute pure feed-forward models with no feed-back mechanisms, which are otherwise known to be important in biological vision. In view of such a background, it is, however, highly interesting to see how well the derived orientation selectivity curves in Figures 2, 4 and 5 reflect the qualitative shapes of the biologically established orientation selectivity curves in Figure 7.

It is also known that the distinction between simple and complex cells may not be as distinct as proposed in the initial work by Hubel and Wiesel, where there could instead be a scale of gradual transitions between simple and complex cells. Considering that the forms of the derived orientation selectivity are often similar for our models of simple and complex cells (as summarized in Table 1), one may speculate that the presented results could be relevant with respect to such a wider contextual background.

In summary, we have with the presented treatment demonstrated how the generalized Gaussian derivative model for visual receptive fields lends itself to closed form theoretical analysis, that can lead to qualitatively very reasonable predictions regarding phenomena in biological vision. We have specifically used these results to support a biological hypothesis concerning expansion of receptive field shapes in the primary visual cortex over the degrees of freedom in natural geometric image transformations, regarding an expansion over the spatial eccentricity (the inverse of the scale parameter ratio κ) of the receptive fields. Based on these results, we specifically propose to also include such an expansion over eccentricity in models of the pinwheel structure of the receptive fields in the visual cortex.

References

E. Adelson and J. Bergen. Spatiotemporal energy models for the perception of motion. *Journal of Optical Society of America, A* 2: 284–299, 1985.

E. Baspinar, G. Citti, and A. Sarti. A geometric model of multi-scale orientation preference maps via Gabor functions. *Journal of Mathematical Imaging and Vision*, 60:900–912, 2018.

P. Berkes and L. Wiskott. Slow feature analysis yields a rich repertoire of complex cell properties. *Journal of Vision*, 5(6):579–602, 2005.

G. G. Blasdel. Orientation selectivity, preference and continuity in monkey striate cortex. *Journal of Neuroscience*, 12(8):3139–3161, 1992.

T. Bonhoeffer and A. Grinvald. Iso-orientation domains in cat visual cortex are arranged in pinwheel-like patterns. *Nature*, 353:429–431, 1991.

R. N. Bracewell. *The Fourier Transform and its Applications*. McGraw-Hill, New York, 1999. 3rd edition.

M. Carandini. What simple and complex cells compute. *The Journal of Physiology*, 577(2):463–466, 2006.

B. R. Conway and M. S. Livingstone. Spatial and temporal properties of cone signals in alert macaque primary visual cortex. *Journal of Neuroscience*, 26(42):10826–10846, 2006.

A. De and G. D. Horwitz. Spatial receptive field structure of double-opponent cells in macaque V1. *Journal of Neurophysiology*, 125(3): 843–857, 2021.

G. C. DeAngelis and A. Anzai. A modern view of the classical receptive field: Linear and non-linear spatio-temporal processing by V1 neurons. In L. M. Chalupa and J. S. Werner, editors, *The Visual Neurosciences*, volume 1, pages 704–719. MIT Press, 2004.

G. C. DeAngelis, I. Ohzawa, and R. D. Freeman. Receptive field dynamics in the central visual pathways. *Trends in Neuroscience*, 18 (10):451–457, 1995.

W. Einhäuser, C. Kayser, P. König, and K. P. Kording. Learning the invariance properties of complex cells from their responses to natural stimuli. *European Journal of Neuroscience*, 15(3):475–486, 2002.

R. C. Emerson, M. C. Citron, W. J. Vaughn, and S. A. Klein. Nonlinear directionally selective subunits in complex cells of cat striate cortex. *Journal of Neurophysiology*, 58(1):33–65, 1987.

M. A. Georgeson, K. A. May, T. C. A. Freeman, and G. S. Hesse. From filters to features: Scale-space analysis of edge and blur coding in human vision. *Journal of Vision*, 7(13):7–, 2007.

R. L. T. Goris, E. P. Simoncelli, and J. A. Movshon. Origin and function of tuning diversity in Macaque visual cortex. *Neuron*, 88(4): 819–831, 2015.

M. Hansard and R. Horoud. A differential model of the complex cell. *Neural Computation*, 23(9):2324–2357, 2011.

T. Hansen and H. Neumann. A recurrent model of contour integration in primary visual cortex. *Journal of Vision*, 8(8):8.1–25, 2008.

D. J. Heeger. Normalization of cell responses in cat striate cortex. *Visual Neuroscience*, 9:181–197, 1992.

G. S. Hesse and M. A. Georgeson. Edges and bars: where do people see features in 1-D images? *Vision Research*, 45(4):507–525, 2005.

D. H. Hubel and T. N. Wiesel. Receptive fields of single neurones in the cat's striate cortex. *J Physiol*, 147:226–238, 1959.

D. H. Hubel and T. N. Wiesel. Receptive fields, binocular interaction and functional architecture in the cat's visual cortex. *J Physiol*, 160: 106–154, 1962.

D. H. Hubel and T. N. Wiesel. *Brain and Visual Perception: The Story of a 25-Year Collaboration*. Oxford University Press, 2005.

E. N. Johnson, M. J. Hawken, and R. Shapley. The orientation selectivity of color-responsive neurons in Macaque V1. *The Journal of Neuroscience*, 28(32):8096–8106, 2008.

J. Jones and L. Palmer. The two-dimensional spatial structure of simple receptive fields in cat striate cortex. *J. of Neurophysiology*, 58:1187–1211, 1987a.

J. Jones and L. Palmer. An evaluation of the two-dimensional Gabor filter model of simple receptive fields in cat striate cortex. *J. of Neurophysiology*, 58:1233–1258, 1987b.

J. J. Koenderink. The structure of images. *Biological Cybernetics*, 50: 363–370, 1984.

J. J. Koenderink and A. J. van Doorn. Representation of local geometry in the visual system. *Biological Cybernetics*, 55:367–375, 1987.

J. J. Koenderink and A. J. van Doorn. Receptive field families. *Biological Cybernetics*, 63:291–298, 1990.

J. J. Koenderink and A. J. van Doorn. Generic neighborhood operators. *IEEE Trans. Pattern Analysis and Machine Intell.*, 14(6):597–605, Jun. 1992.

K. P. Kording, C. Kayser, W. Einhäuser, and P. Konig. How are complex cell properties adapted to the statistics of natural stimuli? *Journal of Neurophysiology*, 91(1):206–212, 2004.

T. Lindeberg. Feature detection with automatic scale selection. *International Journal of Computer Vision*, 30(2):77–116, 1998.

T. Lindeberg. Generalized Gaussian scale-space axiomatics comprising linear scale-space, affine scale-space and spatio-temporal scale-space. *Journal of Mathematical Imaging and Vision*, 40(1):36–81, 2011.

T. Lindeberg. A computational theory of visual receptive fields. *Biological Cybernetics*, 107(6):589–635, 2013.

T. Lindeberg. Time-causal and time-recursive spatio-temporal receptive fields. *Journal of Mathematical Imaging and Vision*, 55(1):50–88, 2016.

T. Lindeberg. Temporal scale selection in time-causal scale space. *Journal of Mathematical Imaging and Vision*, 58(1):57–101, 2017.

T. Lindeberg. Dense scale selection over space, time and space-time. *SIAM Journal on Imaging Sciences*, 11(1):407–441, 2018.

T. Lindeberg. Provably scale-covariant continuous hierarchical networks based on scale-normalized differential expressions coupled in cascade. *Journal of Mathematical Imaging and Vision*, 62(1):120–148, 2020.

T. Lindeberg. Normative theory of visual receptive fields. *Heliyon*, 7(1):e05897:1–20, 2021. doi: 10.1016/j.heliyon.2021.e05897.

T. Lindeberg. Covariance properties under natural image transformations for the generalized Gaussian derivative model for visual receptive fields. *arXiv preprint arXiv:2303.09803*, 2023.

X. Liu and P. A. Robinson. Analytic model for feature maps in the primary visual cortex. *Frontiers in Computational Neuroscience*, 16:2, 2022.

D. G. Lowe. Towards a computational model for object recognition in IT cortex. In *Biologically Motivated Computer Vision*, volume 1811 of *Springer LNCS*, pages 20–31. Springer, 2000.

S. Marcelja. Mathematical description of the responses of simple cortical cells. *Journal of Optical Society of America*, 70(11):1297–1300, 1980.

K. A. May and M. A. Georgeson. Blurred edges look faint, and faint edges look sharp: The effect of a gradient threshold in a multi-scale edge coding model. *Vision Research*, 47(13):1705–1720, 2007.

P. Merolla and K. Boahn. A recurrent model of orientation maps with simple and complex cells. In *Advances in Neural Information Processing Systems (NIPS 2004)*, pages 995–1002, 2004.

J. A. Movshon, E. D. Thompson, and D. J. Tolhurst. Receptive field organization of complex cells in the cat's striate cortex. *The Journal of Physiology*, 283(1):79–99, 1978.

I. Nauhaus, A. Benucci, M. Carandini, and D. L. Ringach. Neuronal selectivity and local map structure in visual cortex. *Neuron*, 57(5):673–679, 2008.

Z.-J. Pei, G.-X. Gao, B. Hao, Q.-L. Qiao, and H.-J. Ai. A cascade model of information processing and encoding for retinal prosthesis. *Neural Regeneration Research*, 11(4):646, 2016.

J. Petitot. The neurogeometry of pinwheels as a sub-Riemannian contact structure. *Journal of Physiology-Paris*, 97(2–3):265–309, 2003.

M. Porat and Y. Y. Zeevi. The generalized Gabor scheme of image representation in biological and machine vision. *IEEE Trans. Pattern Analysis and Machine Intell.*, 10(4):452–468, 1988.

D. L. Ringach. Spatial structure and symmetry of simple-cell receptive fields in macaque primary visual cortex. *Journal of Neurophysiology*, 88:455–463, 2002.

D. L. Ringach. Mapping receptive fields in primary visual cortex. *Journal of Physiology*, 558(3):717–728, 2004.

D. L. Ringach, R. M. Shapley, and M. J. Hawken. Orientation selectivity in macaque V1: Diversity and laminar dependence. *Journal of Neuroscience*, 22(13):5639–5651, 2002.

D. Rose and C. Blakemore. An analysis of orientation selectivity in the cat's visual cortex. *Experimental Brain Research*, 20:1–17, 1974.

N. C. Rust, O. Schwartz, J. A. Movshon, and E. P. Simoncelli. Spatiotemporal elements of macaque V1 receptive fields. *Neuron*, 46(6):945–956, 2005.

P. H. Schiller, B. L. Finlay, and S. F. Volman. Quantitative studies of single-cell properties in monkey striate cortex. II. Orientation specificity and ocular dominance. *Journal of Neurophysiology*, 39(6):1320–1333, 1976.

B. Scholl, A. Y. Y. Tan, J. Corey, and N. J. Priebe. Emergence of orientation selectivity in the mammalian visual pathway. *Journal of Neuroscience*, 33(26):10616–10624, 2013.

T. Serre and M. Riesenhuber. Realistic modeling of simple and complex cell tuning in the HMAX model, and implications for invariant object recognition in cortex. Technical Report AI Memo 2004-017, MIT Computer Science and Artificial Intelligence Laboratory, 2004.

N. V. Swindale. The development of topography in the visual cortex: A review of models. *Network: Computation in Neural Systems*, 7(2):161–247, 1996.

J. Toubyan, B. Lau, and Y. Dan. Isolation of relevant visual features from random stimuli for cortical complex cells. *Journal of Neuroscience*, 22(24):10811–10818, 2002.

J. Toubyan, G. Felsen, and Y. Dan. Spatial structure of complex cell receptive fields measured with natural images. *Neuron*, 45(5):781–791, 2005.

R. L. D. Valois, N. P. Cottaris, L. E. Mahon, S. D. Elfer, and J. A. Wilson. Spatial and temporal receptive fields of geniculate and cortical cells and directional selectivity. *Vision Research*, 40(2):3685–3702, 2000.

S. A. Wallis and M. A. Georgeson. Mach edges: Local features predicted by 3rd derivative spatial filtering. *Vision Research*, 49(14):1886–1893, 2009.

Q. Wang and M. W. Spratling. Contour detection in colour images using a neurophysiologically inspired model. *Cognitive Computation*, 8(6):1027–1035, 2016.

R. A. Young. The Gaussian derivative model for spatial vision: I. Retinal mechanisms. *Spatial Vision*, 2:273–293, 1987.

R. A. Young and R. M. Lesperance. The Gaussian derivative model for spatio-temporal vision: II. Cortical data. *Spatial Vision*, 14(3, 4):321–389, 2001.

R. A. Young, R. M. Lesperance, and W. W. Meyer. The Gaussian derivative model for spatio-temporal vision: I. Cortical model. *Spatial Vision*, 14(3, 4):261–319, 2001.